

# Geochemical Constraints on the Origin of Volcanic Rocks from the Andean Northern Volcanic Zone, Ecuador

J. A. BRYANT<sup>1</sup>, G. M. YOGODZINSKI<sup>1\*</sup>, M. L. HALL<sup>2</sup>, J. L. LEWICKI<sup>3</sup>  
AND D. G. BAILEY<sup>4</sup>

<sup>1</sup>DEPARTMENT OF GEOLOGICAL SCIENCES, UNIVERSITY OF SOUTH CAROLINA, 701 SUMTER STREET, COLUMBIA, SC 29208, USA

<sup>2</sup>INSTITUTO GEOFISICO, ESCUELA POLITECNICA NACIONAL (IG-EPN), APARTADO 17-01-2759 QUITO, ECUADOR

<sup>3</sup>EARTH SCIENCES DIVISION, LAWRENCE-BERKELEY NATIONAL LABORATORY, 1 CYCLOTRON ROAD, MAIL STOP 90-1116, BERKELEY, CA 94720, USA

<sup>4</sup>DEPARTMENT OF GEOSCIENCES, HAMILTON COLLEGE, CLINTON, NY 13323, USA

RECEIVED JULY 25, 2004; ACCEPTED JANUARY 27, 2006  
ADVANCE ACCESS PUBLICATION MARCH 7, 2006

*Whole-rock geochemical data on basaltic to rhyolitic samples from 12 volcanic centers are used to constrain the role of continental crust in the genesis of magmas formed beneath the anomalously wide subduction-related volcanic arc in Ecuador. Relatively homogeneous, mantle-like, isotopic compositions across the arc imply that the parental magmas in Ecuador were produced largely within the mantle wedge above the subduction zone and not by extensive melting of crustal rocks similar to those upon which the volcanoes were built. Cross-arc changes in  $^{143}\text{Nd}/^{144}\text{Nd}$  and  $\Delta 7/4\text{Pb}$  are interpreted to result from assimilation of geochemically mature continental crust, especially in the main arc area, 330–360 km from the trench. Mixing calculations limit the quantity of assimilated crust to less than ~10%. Most andesites and dacites in Ecuador have adakite-like trace element characteristics (e.g.  $\text{Y} < 18 \text{ ppm}$ ,  $\text{Yb} < 2 \text{ ppm}$ ,  $\text{La}/\text{Yb} > 20$ ,  $\text{Sr}/\text{Y} > 40$ ). Available whole-rock data do not provide a clear basis for distinguishing between slab-melting and deep crustal fractionation models for the genesis of Ecuador adakites; published data highlighting geochemical evolution within individual volcanoes, and in magmatic rocks produced throughout Ecuador since the Eocene, appear to support the deep fractionation model for the genesis of most evolved Ecuadorian lavas. A subset of andesites, which display a combination of high Sr ( $> 900 \text{ ppm}$ ),  $\epsilon\text{Nd} > 4.1$  and  $\Delta 7/4\text{Pb} < 6.0$ , appear to be the best candidates among Ecuador lavas for slab-melts associated with the subduction of the relatively young, over-thickened, oceanic crust of the Carnegie Ridge.*

KEY WORDS: andesite; Ecuador; trace elements; isotopes; adakite

## INTRODUCTION

It is widely believed that subduction-related andesites form predominantly through the differentiation of basaltic melts and their interaction with arc crust (e.g. Gill, 1981; James & Murcia, 1984). In oceanic settings, where the arc crust is thin, the contribution of crustal material to the formation of lavas is often minimal, and andesites are viewed as secondary products of basalt evolution by crystal fractionation and magma mixing (Gill, 1981; Conrad & Kay, 1984; Woodhead, 1988; Singer & Myers, 1990). This model for andesite genesis in island arcs is central to our understanding of subduction zone magmatism, and has played a significant role in the development of ideas on the formation and evolution of continental crust in subduction zones (e.g. Kay & Kay, 1991; Kelemen, 1995).

An alternative view of arc magmatism and andesite genesis has recently grown out of the recognition that in some arcs, especially in places where the subducting lithosphere is young and/or warm, calc-alkaline andesites and dacites may form not only through the differentiation of basaltic magmas, but also through partial melting of basaltic rocks at high pressures in subducting oceanic

\*Corresponding author. Telephone: 001-803-777-9524. Fax: 001-803-777-6610. E-mail: gyogodzins@geol.sc.edu

crust (Kay, 1978; Saunders *et al.*, 1987; Defant & Drummond, 1990; Kay *et al.*, 1993; Yogodzinski *et al.*, 1995; Stern & Killian, 1996; Rapp *et al.*, 1999; Kelemen *et al.*, 2003). Andesites and dacites thought to have formed by this mechanism have unusual trace element characteristics, including high Sr/Y (>40) and La/Yb (>20), and low concentrations of Y (<18 ppm) and Yb (<1.9 ppm) compared with common island arc lavas of intermediate composition (Defant & Drummond, 1990). The geochemically distinctive class of andesites and dacites with these features, now commonly termed 'adakites' (Defant & Drummond, 1990), was first recognized by Kay (1978), who argued that they were formed through a two-step process that involved melting of the subducting oceanic crust in the presence of garnet (to produce the highly fractionated trace element patterns), followed by the interaction of the resulting silicic melt with peridotite in the hot mantle wedge (to form the andesitic and high Mg-number characteristics).

This model has been relatively successful in explaining the genesis of adakitic lavas in island arcs or other arc settings where the crust is relatively thin (Saunders *et al.*, 1987; Defant *et al.*, 1991; Morris, 1995; Yogodzinski *et al.*, 1995; Stern & Killian, 1996; Abratis & Wörner, 2001). Recently however, the model has been applied in areas of thickened continental crust, where the mineral garnet, which plays the central role in generating the highly fractionated trace element patterns seen in adakites (Kay, 1978; Defant & Drummond, 1990; Rapp *et al.*, 1999), may be stable not only in the subducting oceanic plate, but also in the deep crust (e.g. Gutscher *et al.*, 2000; Beate *et al.*, 2001; Bourdon *et al.*, 2002, 2003). Not surprisingly, studies in this geological setting, in particular in Ecuador, have produced a divergence of opinions, with some researchers focusing on the crust as a major component of northern Andean magmatism (Kilian & Pichler, 1989; Arculus *et al.*, 1999; Monzier *et al.*, 1999), and others advocating processes within the subducting slab and mantle wedge (Barragan *et al.*, 1998; Gutscher *et al.*, 1999; Bourdon *et al.*, 2002, 2003). Reconciliation of this issue will ultimately determine the extent to which we view widespread andesite–dacite volcanism in the northern Andes as juvenile additions to the continental crust, or as recycling of old crust via intra-crustal melting and differentiation.

In this paper we present whole-rock geochemical data, including Pb, Sr, and Nd isotope ratios, for Holocene and Late Pleistocene lavas collected from most of the length and width of the volcanic arc in Ecuador. Because the crust varies greatly in thickness and composition across the arc, from primitive oceanic terranes in the west (basalts and related volcanoclastic rocks) to geochemically mature continental lithologies in the east (granites and metapelites), these data provide a potentially powerful basis for evaluating the role of crustal melting and

assimilation in the genesis of adakitic and other volcanic rocks in Ecuador.

## GEOLOGICAL SETTING

The spatial distribution of active volcanism in the northern Andes, which is controlled by the convergence of the Nazca and South American plates, undergoes a dramatic series of along-strike changes from central Colombia southward into northern Peru (Fig. 1). In southern Colombia, the arc is a relatively narrow volcanic chain (40–50 km wide), which is underlain by subducting oceanic lithosphere that dips to the SE at an angle of  $\sim 30^\circ$  (Gutscher *et al.*, 1999). In northernmost Ecuador, the volcanic arc widens abruptly to  $\sim 120$  km, but ends a short distance to the south at Sangay Volcano, in central Ecuador (Fig. 1). In southernmost Ecuador and northern Peru, the subduction zone enters the non-volcanic/flat-slab region (Barazangi & Isacks, 1976). The abrupt widening of the volcanic arc and the southward cessation of active volcanism in Ecuador coincides spatially with the impingement of the 14 km thick crust of the Carnegie Ridge (Graindorge *et al.*, 2004) on the South American margin (Fig. 1). Landward of this point, the dip of the subducting plate beneath Ecuador is  $25\text{--}30^\circ$ , similar to the dip of the subducting plate beneath southern Colombia to the north (Guillier *et al.*, 2001). These observations suggest that the deep structure of the subducting Carnegie Ridge exerts some control over the surface expression of active volcanism in the Northern Andes (note in particular the widening of the volcanic arc in Ecuador, Fig. 1), even though the dip of the subducting plate appears to change very little from southern Colombia to central and southern Ecuador (Gutscher *et al.*, 1999; Guillier *et al.*, 2001).

The north Andean crust that underlies the currently active volcanoes in Colombia and Ecuador varies systematically across the margin with respect to thickness, age, rock type and geochemical maturity (Fig. 2). Estimates based on gravity data indicate that the crustal thickness across Ecuador changes from 25–30 km beneath the volcanic front to >50 km beneath the highest elevations of the Eastern Cordillera, with progressive thinning of the basement eastward toward the craton (Feininger & Seguin, 1983). In Colombia, gravity data indicate that the crust is 45–50 km thick along the axis of the Andes and that it thins to 32–35 km towards both the craton and the coast (Salvador, 1991). Recent seismic data have been interpreted to indicate that the crust is 40–50 km thick beneath western Ecuador, and perhaps 50–75 km thick beneath the arc crest (Prévoit *et al.*, 1996; Guillier *et al.*, 2001).

The geological settings of individual volcanoes in Ecuador can be divided into three cross-arc zones,

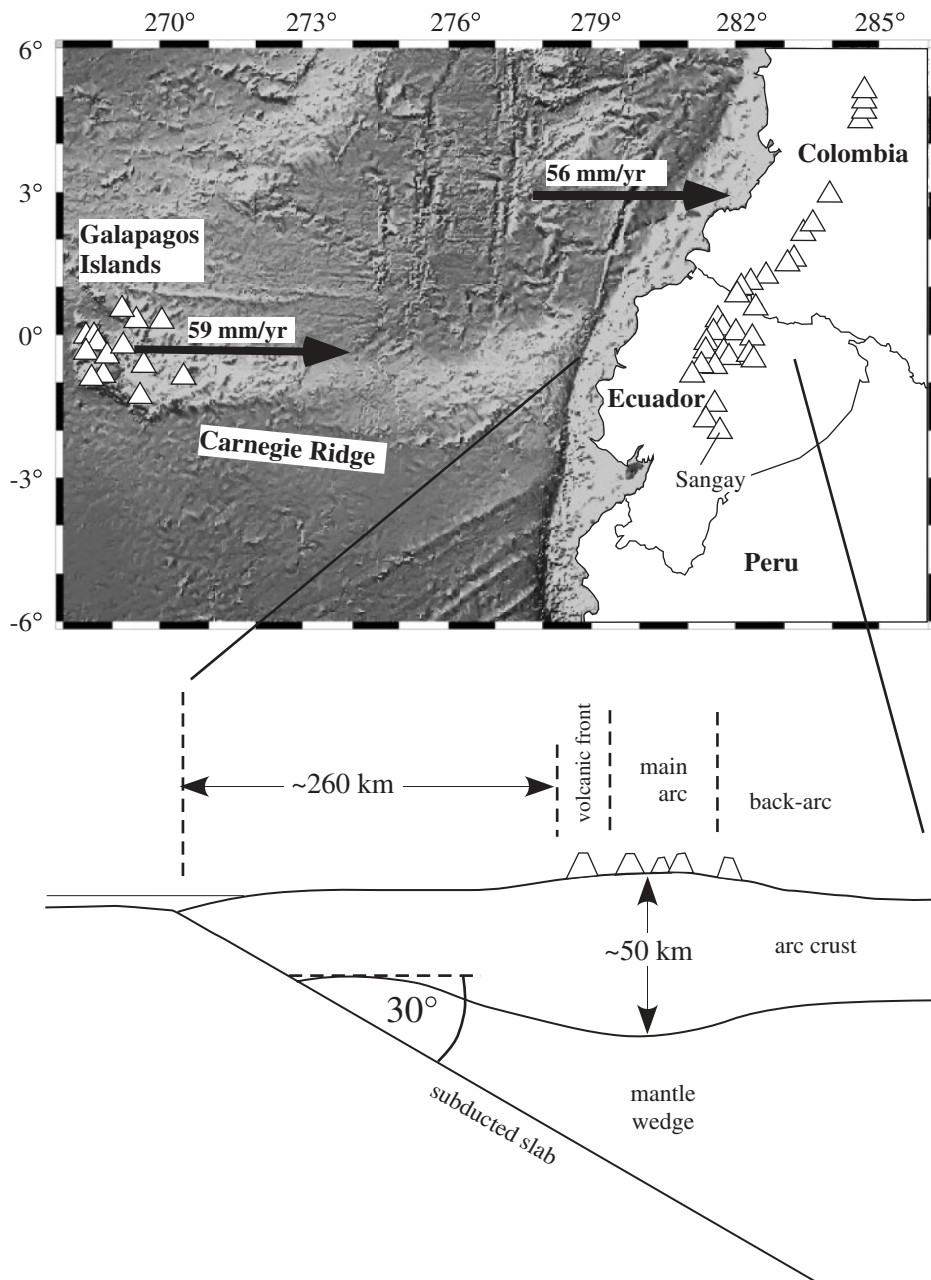
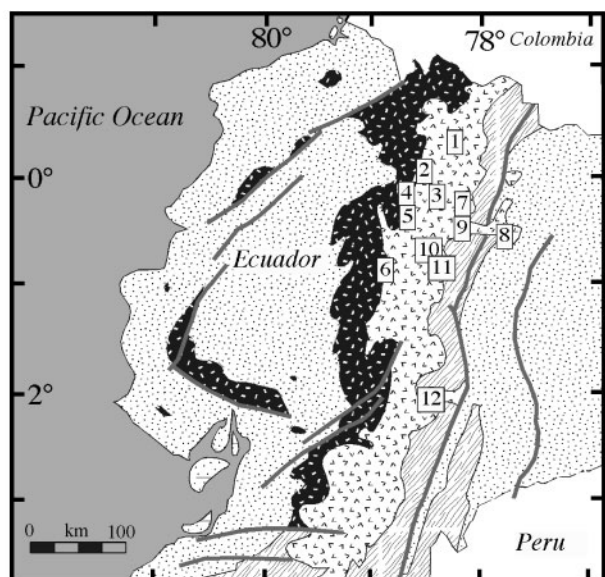


**Fig. 1.** Topographic (onshore) and bathymetric (offshore) map of the Northern Andes region, showing the major geographical features mentioned in the text.  $\Delta$ , locations of Quaternary volcanoes from the Smithsonian Global Volcanism database. Black arrows show the convergence direction and rate of movement of the Nazca Plate relative to stable South America from Trenkamp *et al.* (2002). Crustal thickness estimate (50 km) is a minimum value based on the work of Prévot *et al.* (1996) and Guillier *et al.* (2001). Average dip of 30° for the subducting slab beneath Ecuador is from Guillier *et al.* (2001).

based on their distance from the trench and on the age, composition, and thickness of the crust upon which they were built (Figs 1 and 2). We refer to these zones as (1) the volcanic front, which lies in the Western Cordillera, 260–300 km from the trench, (2) the main arc, which encompasses the Inter-Andean Graben and Eastern Cordillera

and lies 300–380 km from the trench, and (3) the back-arc area, which lies in the eastern foothills of the Northern Andes at distances greater than ~380 km from the trench (Fig. 1).

Surface exposures of basement rocks at the volcanic front are composed primarily of geochemically primitive





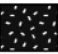


Geologic Units		Volcanic Centers	
	Foreland & Forearc Sedimentary Cover (Tertiary-Quaternary)	Imbabura	1
	Continental Volcanic Arc (Tertiary-Quaternary)	Pululagua	2
	Oceanic & Island Arc Terranes (Cretaceous-Paleocene)	Ilalo	3
	Igneous & Metamorphic Basement (Paleozoic-Mesozoic)	Pichincha	4
	Major Faults	Atacazo	5
		Quilotoa	6
		Chacana	7
		Sumaco	8
		Antisana	9
		Cotopaxi	10
		Chalupas	11
		Sangay	12

Fig. 2. Simplified geological map of Ecuador, modified from Jaillard *et al.* (1997). Samples for this study include basalts, andesites, dacites and rhyolites from 12 volcanic centers (numbered in boxes) across the 120 km width of the arc.

oceanic basalts and volcanoclastic rocks that were accreted to the northern Andean margin since the mid-Cretaceous. These oceanic terranes include fragments of the Caribbean Plateau as well as geochemically primitive, island-arc-type crustal blocks (Fig. 2; e.g. Feininger, 1987; Megard, 1989; Jaillard *et al.*, 1990, 1997; Reynaud *et al.*, 1999; Hughes & Pilatasig, 2002; Kerr & Tarney, 2005). The geochemistry of the oceanic basalts is broadly similar to those of the Galapagos and the Carnegie Ridge (Dupré & Echeverria, 1984; Lapiere *et al.*, 2000; Kerr *et al.*, 2002, 2004; Mamberti *et al.*, 2003). To the east, the crust beneath the main arc and back-arc becomes progressively older on average, and geochemically more mature, consisting increasingly of granites, schists, and gneisses of mostly late Mesozoic to Paleozoic age (Fig. 2; Aspdén *et al.*, 1992; Aspdén & Litherland, 1992; Litherland *et al.*, 1994; Noble *et al.*, 1997). Beneath

the back-arc of Ecuador, the volcanoes appear to lie above Precambrian basement. Precambrian rocks are absent from surface exposures, but have been recovered in cuttings from deep oil wells (Feininger, 1987).

## ANALYTICAL METHODS

Whole-rock major and trace element concentrations were determined from fresh samples that were crushed in a steel jaw crusher and ground in agate or Al-ceramic containers. Major elements and some trace elements (Ni, Cr, Cu, V) were determined by X-ray fluorescence (XRF) at the Washington State Geoanalytical Laboratory on a low dilution Li-tetraborate fused bead (Johnson *et al.*, 1999). Major elements are reported on an anhydrous basis with totals normalized to 100% (Table 1). The remaining trace element concentrations were measured by inductively coupled plasma mass spectrometry (ICP-MS), also at Washington State University. Techniques for ICP-MS sample preparation, instrument operation, and calibrations have been described by Lichte *et al.* (1987). Major element data for samples from Sumaco, Atacazo, and Antisana are from Barragan *et al.* (1998). Isotope ratios for Sr, Nd, and Pb were determined by thermal ionization mass spectrometry at the University of North Carolina, Chapel Hill. All samples were dissolved at the University of South Carolina in high-purity HNO<sub>3</sub> and HF for 3 days in steel-jacketed Teflon capsules in an oven at 155°C. Chemical separates of Sr and Nd were made from the aliquoted sample by cation exchange using Sr-spec and HDEP-coated Teflon cation-exchange resins. Lead was separated by anion exchange using HBr. The Sr and Nd data are normalized to  $^{86}\text{Sr}/^{88}\text{Sr} = 0.1194$  and  $^{146}\text{Nd}/^{144}\text{Nd} = 0.7219$ , assuming exponential fractionation behavior. The Pb data are corrected for 0.12%/a.m.u. fractionation relative to Pb isotope standard NBS981. Errors on Pb isotope ratios ( $^{206}\text{Pb}/^{204}\text{Pb} = \pm 0.023$ ,  $^{207}\text{Pb}/^{204}\text{Pb} = \pm 0.028$ ,  $^{208}\text{Pb}/^{204}\text{Pb} = \pm 0.093$ ,  $2\sigma$  absolute on all data in Table 2) are dominated by fractionation uncertainty of 0.06%/a.m.u. Seventy-two runs of the NBS-987 isotope standard yielded an average  $^{87}\text{Sr}/^{86}\text{Sr}$  value of  $0.710263 \pm 0.000009$  ( $2\sigma$ ). Data listed in Table 2 are corrected to a value of 0.710240 for NBS-987. Twenty runs of the JNdi-1 isotope standard solution yielded an average  $^{143}\text{Nd}/^{144}\text{Nd}$  value of  $0.512110 \pm 0.000016$  ( $2\sigma$ ). Data in Table 2 are corrected to a  $^{143}\text{Nd}/^{144}\text{Nd}$  value of 0.512115 for JNdi-1, consistent with a CHUR value of 0.512635 and an  $\epsilon\text{Nd}$  value of  $-15.15$  for the La Jolla Nd standard, and implying an  $\epsilon\text{Nd}$  value of  $-10.13$  for the JNdi-1 standard (Lugmair & Carlson, 1978; Wasserburg *et al.*, 1981; Tanaka *et al.*, 2000). Errors on  $^{143}\text{Nd}/^{144}\text{Nd}$  and  $^{87}\text{Sr}/^{86}\text{Sr}$  reported in Table 2 are internal-run precision only. Isotopic measurements were collected primarily in the 9 month period that began in January 2002.

Table 1: Whole-rock major element (wt %) and trace element (ppm) compositions of Ecuador lavas

Sample:	lmb-1	lmb-2	lmb-3	lmb-4	lmb-11	lmb-14	lmb-16	lmb-21.2	lmb-22
Center:	lmbabura	lmbabura	lmbabura	lmbabura	lmbabura	lmbabura	lmbabura	lmbabura	lmbabura
Rock type:	andesite	andesite	andesite	andesite	andesite	andesite	andesite	dacite	andesite
SiO <sub>2</sub>	59.84	57.76	59.42	60.10	59.30	61.74	61.87	63.46	56.86
TiO <sub>2</sub>	0.58	0.63	0.59	0.54	0.59	0.48	0.48	0.52	0.67
Al <sub>2</sub> O <sub>3</sub>	17.80	17.00	17.74	17.84	17.51	17.73	17.66	16.65	17.91
FeO*	5.84	6.85	6.07	6.18	6.32	5.46	5.46	5.00	7.18
MnO	0.11	0.12	0.12	0.13	0.12	0.12	0.12	0.09	0.12
MgO	3.54	5.11	3.66	3.17	3.68	2.66	2.60	2.90	4.58
CaO	7.00	7.80	7.14	7.25	7.27	6.65	6.63	5.77	7.69
Na <sub>2</sub> O	3.67	3.59	3.71	3.63	3.71	3.92	3.95	4.00	3.86
K <sub>2</sub> O	1.41	0.99	1.33	0.94	1.26	1.04	1.03	1.48	0.99
P <sub>2</sub> O <sub>5</sub>	0.21	0.15	0.23	0.22	0.23	0.20	0.21	0.13	0.15
Rb	21.3	16.1	21.1	14.9	17.9	17.1	16.2	28.2	17.8
Sr	1051	475	1109	785	978	783	745	462	518
Y	15.7	12.9	15.8	16.2	16.0	15.2	14.5	10.3	13.3
Zr	86	73	87	77	79	85	82	75	76
Nb	3.17	2.66	3.18	3.11	2.98	3.06	2.95	2.55	2.43
Cs	1.19	0.53	1.17	0.60	0.92	0.66	0.63	1.03	0.62
Ba	813	433	858	448	705	515	498	614	467
Hf	2.55	2.06	2.51	2.27	2.36	2.43	2.29	2.20	2.17
Ta	0.19	0.18	0.20	0.20	0.19	0.18	0.18	0.20	0.15
Pb	12.6	4.32	12.5	6.41	9.96	6.28	6.17	4.94	4.51
Th	8.55	1.40	8.89	3.22	7.05	3.53	3.35	1.38	1.34
U	2.63	0.52	2.68	1.09	2.16	1.13	1.09	0.70	0.56
Sc	19	24	20	16	19	13	13	14	24
V	116	165	131	124	143	112	106	110	171
Cr	27	101	36	17	29	22	16	63	33
Ni	17	47	19	9	15	9	10	18	23
Cu	43	44	33	33	31	22	25	17	32
Zn	77	76	74	77	76	72	72	72	77
La	22.9	8.52	23.2	13.6	20.4	14.2	13.6	7.62	7.81
Ce	39.2	16.5	40.1	25.4	35.8	26.3	25.2	14.5	15.4
Pr	4.59	2.09	4.67	3.17	4.24	3.22	3.06	1.88	2.04
Nd	18.9	9.33	19.5	13.8	17.7	13.6	13.1	8.34	9.32
Sm	3.95	2.50	4.04	3.12	3.79	3.05	2.95	2.25	2.52
Eu	1.15	0.81	1.21	0.99	1.13	0.97	0.90	0.73	0.85
Gd	3.17	2.49	3.23	2.92	3.21	2.63	2.57	2.13	2.47
Tb	0.46	0.39	0.48	0.48	0.47	0.42	0.41	0.32	0.40
Dy	2.82	2.35	2.87	2.89	2.84	2.68	2.55	1.90	2.49
Ho	0.59	0.48	0.59	0.59	0.58	0.53	0.53	0.37	0.51
Er	1.55	1.26	1.61	1.59	1.63	1.51	1.44	1.00	1.36
Tm	0.23	0.18	0.23	0.23	0.24	0.23	0.21	0.14	0.19
Yb	1.51	1.15	1.50	1.47	1.52	1.43	1.38	0.89	1.22
Lu	0.24	0.18	0.24	0.24	0.24	0.23	0.22	0.15	0.19

Table 1: continued

Sample:	lmb-26	lmb-28	lmb-29	lmb-30	lmb-32	lmb-36	lmb-38	lmb-39	lmb-42
Center:	lmbabura	lmbabura	lmbabura	lmbabura	lmbabura	lmbabura	lmbabura	lmbabura	lmbabura
Rock type:	andesite	andesite	andesite	andesite	andesite	andesite	andesite	andesite	andesite
SiO <sub>2</sub>	60.18	60.90	60.26	58.67	58.10	60.09	59.13	60.00	62.47
TiO <sub>2</sub>	0.51	0.51	0.53	0.70	0.58	0.53	0.68	0.54	0.45
Al <sub>2</sub> O <sub>3</sub>	16.36	16.55	16.20	17.08	16.76	17.60	17.06	17.93	17.02
FeO*	5.83	5.60	5.93	6.26	6.49	6.15	5.95	6.18	5.27
MnO	0.11	0.10	0.11	0.11	0.11	0.13	0.11	0.13	0.11
MgO	5.13	4.59	5.27	4.79	5.59	3.38	4.66	3.14	3.21
CaO	6.78	6.72	6.80	7.06	7.54	7.17	6.85	7.24	6.25
Na <sub>2</sub> O	3.71	3.69	3.63	3.69	3.65	3.66	3.95	3.73	3.83
K <sub>2</sub> O	1.28	1.21	1.15	1.46	1.03	1.09	1.42	0.91	1.26
P <sub>2</sub> O <sub>5</sub>	0.12	0.12	0.13	0.19	0.13	0.22	0.19	0.20	0.13
Rb	23.3	21.3	24.2	27.3	19.9	15.6	28.2	13.5	25.5
Sr	456	442	438	555	430	832	518	727	440
Y	10.8	10.4	12.1	11.4	11.0	14.6	10.9	14.6	11.3
Zr	67	69	76	89	68	69	86	72	76
Nb	2.32	2.68	2.75	3.89	2.14	2.72	3.78	2.94	2.75
Cs	0.72	0.73	0.84	0.81	0.41	0.76	0.74	0.51	0.90
Ba	504	501	515	586	426	495	545	416	556
Hf	1.91	1.98	2.14	2.47	1.95	2.05	2.41	2.10	2.18
Ta	0.17	0.17	0.20	0.25	0.14	0.16	0.24	0.18	0.20
Pb	5.35	4.54	5.55	6.04	4.27	7.23	5.87	5.57	5.83
Th	1.95	2.18	2.03	2.62	1.55	3.65	2.70	2.78	2.03
U	0.67	0.57	0.75	0.72	0.57	1.32	0.78	0.95	0.79
Sc	22	22	19	19	25	18	19	16	16
V	141	137	144	146	158	132	158	122	107
Cr	228	200	260	182	163	20	147	21	73
Ni	75	56	65	52	55	11	45	13	22
Cu	30	31	26	44	40	36	39	44	17
Zn	69	71	67	73	72	74	70	75	66
La	7.77	8.18	8.89	13.1	7.29	14.1	12.7	13.0	9.32
Ce	14.8	15.5	16.9	25.1	14.2	25.9	24.0	24.0	17.4
Pr	1.83	1.91	2.06	3.08	1.80	3.18	2.87	3.11	2.11
Nd	8.03	8.25	8.98	13.1	8.03	13.4	12.2	13.0	8.83
Sm	2.05	2.13	2.22	3.16	2.12	3.07	2.88	2.92	2.11
Eu	0.68	0.70	0.73	0.97	0.70	0.96	0.86	0.94	0.69
Gd	1.95	2.01	2.16	2.78	2.15	2.66	2.53	2.67	2.04
Tb	0.32	0.32	0.35	0.40	0.34	0.41	0.37	0.42	0.33
Dy	1.98	1.99	2.10	2.32	2.05	2.54	2.16	2.59	1.99
Ho	0.40	0.40	0.43	0.44	0.42	0.53	0.40	0.52	0.40
Er	1.11	1.05	1.20	1.10	1.12	1.45	1.04	1.45	1.14
Tm	0.16	0.15	0.18	0.15	0.16	0.21	0.14	0.21	0.17
Yb	1.03	0.93	1.11	0.93	0.99	1.34	0.87	1.37	1.04
Lu	0.15	0.15	0.17	0.15	0.16	0.22	0.13	0.21	0.17

Sample:	Imb-45	Pul-1	Pul-2	Pul-3	Pul-4	Pul-5	Pul-6	Pul-7	Pul-8
Center:	Imbabura	Pululagua	Pululagua	Pululagua	Pululagua	Pululagua	Pululagua	Pululagua	Pululagua
Rock type:	andesite	dacite	dacite	dacite	dacite	andesite	dacite	dacite	dacite
SiO <sub>2</sub>	61.70	63.49	63.37	63.06	63.28	62.69	63.68	63.67	63.37
TiO <sub>2</sub>	0.48	0.57	0.57	0.57	0.57	0.54	0.52	0.54	0.55
Al <sub>2</sub> O <sub>3</sub>	17.85	16.56	16.54	16.75	16.67	16.29	16.29	16.96	16.69
FeO*	5.32	5.55	5.63	5.50	5.53	5.36	5.18	5.05	5.39
MnO	0.12	0.09	0.09	0.09	0.09	0.10	0.09	0.08	0.08
MgO	2.71	2.75	2.68	2.85	2.75	3.58	3.12	2.58	2.77
CaO	6.71	5.40	5.41	5.58	5.49	5.77	5.34	5.36	5.37
Na <sub>2</sub> O	3.87	4.40	4.51	4.42	4.44	4.37	4.41	4.57	4.57
K <sub>2</sub> O	1.04	1.05	1.07	1.05	1.06	1.17	1.24	1.04	1.06
P <sub>2</sub> O <sub>5</sub>	0.20	0.14	0.14	0.14	0.14	0.13	0.13	0.15	0.15
Rb	15.8	15.9	17.1	16.5	16.2	20.4	22.0	16.3	16.1
Sr	720	386	425	416	419	399	397	466	451
Y	13.9	11.6	12.3	12.0	11.7	13.2	12.7	9.70	10.4
Zr	77	76	83	79	79	90	97	79	78
Nb	2.82	2.87	3.12	2.94	2.95	3.04	3.24	2.70	2.73
Cs	0.58	0.35	0.45	0.56	0.48	0.34	0.47	0.42	0.57
Ba	466	467	517	485	494	540	576	465	463
Hf	2.20	2.27	2.52	2.38	2.41	2.58	2.76	2.38	2.35
Ta	0.17	0.20	0.22	0.20	0.21	0.22	0.24	0.19	0.19
Pb	5.87	3.99	4.31	3.93	4.12	4.79	4.83	4.19	4.16
Th	3.06	0.95	1.04	1.00	1.02	1.43	1.58	0.96	0.96
U	1.02	0.46	0.49	0.47	0.48	0.62	0.66	0.45	0.47
Sc	14	16	16	16	15	18	16	13	14
V	114	121	129	126	125	120	114	111	120
Cr	17	26	31	33	32	121	96	35	35
Ni	7	16	11	16	16	35	28	15	16
Cu	25	28	27	26	23	25	28	22	30
Zn	73	75	75	77	74	68	69	72	75
La	13.2	7.75	8.01	7.41	7.77	8.58	9.17	7.83	7.68
Ce	24.5	15.3	16.4	15.5	15.6	16.2	17.1	15.5	15.5
Pr	3.00	2.17	2.22	2.09	2.07	2.11	2.21	2.04	2.05
Nd	12.8	9.88	10.0	9.49	9.40	9.39	9.60	9.28	9.45
Sm	2.81	2.58	2.68	2.55	2.57	2.46	2.46	2.40	2.47
Eu	0.91	0.78	0.83	0.82	0.81	0.74	0.74	0.77	0.75
Gd	2.55	2.51	2.64	2.52	2.51	2.40	2.38	2.24	2.37
Tb	0.39	0.39	0.40	0.39	0.38	0.39	0.39	0.34	0.35
Dy	2.41	2.22	2.36	2.25	2.26	2.38	2.27	1.89	1.97
Ho	0.49	0.43	0.46	0.44	0.43	0.47	0.46	0.36	0.39
Er	1.37	1.14	1.21	1.16	1.10	1.29	1.28	0.95	0.99
Tm	0.20	0.16	0.17	0.16	0.16	0.19	0.18	0.13	0.14
Yb	1.30	0.98	0.99	1.00	0.99	1.22	1.18	0.81	0.84
Lu	0.21	0.15	0.16	0.16	0.16	0.20	0.18	0.12	0.14

Table 1: continued

Sample:	Pul-9	Pul-10	Pul-11	Pul-12	QI-12	CI-11	Ch-3	Ch-4	Ch-5
Center:	Pululagua	Pululagua	Pululagua	Pululagua	Quilotoa	Chalupas	Chacana	Chacana	Chacana
Rock type:	andesite	andesite	andesite	andesite	dacite	rhyolite	andesite	rhyolite	rhyolite
SiO <sub>2</sub>	61.34	61.93	61.91	62.29	65.98	74.46	57.78	77.23	74.57
TiO <sub>2</sub>	0.62	0.63	0.61	0.61	0.46	0.24	0.78	0.15	0.21
Al <sub>2</sub> O <sub>3</sub>	15.91	16.16	16.30	16.32	16.99	14.13	16.20	12.79	14.22
FeO*	6.34	6.27	6.13	5.48	3.51	1.24	6.90	0.78	1.09
MnO	0.10	0.10	0.10	0.09	0.07	0.05	0.12	0.05	0.06
MgO	4.38	3.85	3.74	3.88	2.00	0.38	6.40	0.16	0.28
CaO	6.02	5.70	5.78	5.87	4.53	1.26	7.23	0.38	1.20
Na <sub>2</sub> O	4.06	4.20	4.22	4.24	4.68	3.58	3.18	4.24	4.38
K <sub>2</sub> O	1.07	1.04	1.05	1.07	1.62	4.63	1.27	4.19	3.95
P <sub>2</sub> O <sub>5</sub>	0.15	0.13	0.15	0.15	0.16	0.04	0.13	0.03	0.04
Rb	16.4	15.9	15.7	15.9	30.9	182	34.3	125	126
Sr	423	429	424	436	533	221	399	33.0	236
Y	12.2	11.6	12.1	11.6	8.87	12.8	13.3	16.3	10.2
Zr	79	81	80	79	88	169	77	106	145
Nb	2.64	2.73	2.75	2.68	3.47	11.6	4.42	12.1	11.2
Cs	0.60	0.62	0.59	0.58	1.65	9.77	0.91	5.87	5.45
Ba	444	454	449	448	589	1047	442	1082	1096
Hf	2.28	2.37	2.30	2.34	2.59	5.25	2.32	3.81	4.22
Ta	0.18	0.18	0.18	0.17	0.29	1.23	0.39	1.02	1.10
Pb	4.09	4.47	4.48	4.10	7.99	23.2	6.07	19.8	19.9
Th	1.04	1.06	1.05	1.05	3.55	21.5	4.23	12.8	15.6
U	0.47	0.48	0.48	0.49	1.39	9.12	1.66	4.32	5.67
Sc	20	18	19	19	8	2	24	3	2
V	145	143	140	144	85	10	182	5	12
Cr	147	103	87	100	14	0	246	0	0
Ni	37	32	29	31	15	2	93	4	3
Cu	9	20	31	23	23	5	45	3	4
Zn	78	77	80	80	63	39	77	45	37
La	7.37	7.47	7.40	7.58	12.1	32.2	10.3	20.4	31.3
Ce	15.0	15.0	15.2	15.5	22.9	53.7	20.0	38.1	51.5
Pr	2.01	2.00	2.04	1.99	2.77	5.60	2.45	4.28	5.08
Nd	9.24	9.10	9.44	9.20	11.4	19.6	10.4	15.0	16.9
Sm	2.51	2.42	2.52	2.45	2.58	3.52	2.77	3.49	2.90
Eu	0.79	0.78	0.81	0.76	0.74	0.64	0.92	0.43	0.61
Gd	2.50	2.46	2.55	2.42	2.18	2.64	2.72	2.74	2.05
Tb	0.39	0.37	0.39	0.37	0.30	0.39	0.44	0.49	0.31
Dy	2.36	2.21	2.23	2.18	1.69	2.27	2.62	2.96	1.73
Ho	0.45	0.44	0.45	0.41	0.33	0.43	0.52	0.57	0.35
Er	1.23	1.18	1.18	1.12	0.81	1.21	1.37	1.54	0.97
Tm	0.18	0.17	0.17	0.16	0.12	0.18	0.20	0.25	0.15
Yb	1.09	1.02	1.03	1.01	0.72	1.28	1.20	1.58	1.02
Lu	0.17	0.17	0.17	0.16	0.11	0.20	0.19	0.24	0.16



Sample:	Ch-6	Ch-7	Ch-8	Il-2	GS4†	3D3†	GS5†	Cx-9	Cx-10
Center:	Chacana	Chacana	Chacana	Ilalo	Sumaco	Sumaco	Sumaco	Cotopaxi	Cotopaxi
Rock type:	andesite	andesite	dacite	andesite	bas-and	basalt	bas-and	rhyolite	rhyolite
SiO <sub>2</sub>	62.40	62.19	63.11	57.33	54.02	43.24	54.22	73.98	71.96
TiO <sub>2</sub>	0.72	0.80	0.76	0.79	0.78	1.72	0.77	0.19	0.25
Al <sub>2</sub> O <sub>3</sub>	17.12	16.42	16.62	17.24	19.39	15.82	19.67	14.87	15.62
FeO*	4.95	4.97	4.64	7.05	6.30	11.62	6.51	1.28	1.81
MnO	0.08	0.09	0.08	0.13	0.22	0.23	0.22	0.08	0.08
MgO	2.69	3.14	2.65	5.41	1.77	6.31	1.77	0.45	0.61
CaO	5.53	5.57	5.22	7.16	6.31	14.20	6.09	1.67	2.31
Na <sub>2</sub> O	4.15	4.21	4.24	3.71	6.62	4.43	6.33	4.56	4.57
K <sub>2</sub> O	2.14	2.34	2.43	1.02	4.12	1.05	3.96	2.83	2.66
P <sub>2</sub> O <sub>5</sub>	0.22	0.27	0.26	0.16	0.47	1.38	0.46	0.09	0.12
Rb	61.3	61.5	59.9	16.3	106	97.7	108	71.4	63.6
Sr	609	777	749	515	2597	2582	2560	288	353
Y	11.6	12.3	11.5	12.3	38.4	41.9	37.5	10.0	10.5
Zr	127	114	127	79	359	231	353	119	128
Nb	5.77	8.72	8.23	2.92	54.3	37.9	53.4	7.39	6.50
Cs	1.57	2.54	2.22	0.29	2.79	1.70	2.84	2.75	2.67
Ba	822	819	1021	471	2797	1435	2800	878	912
Hf	3.57	3.37	3.56	2.27	6.87	5.39	6.82	3.50	3.61
Ta	0.40	0.69	0.60	0.19	2.98	1.94	2.95	0.68	0.53
Pb	11.2	11.8	12.2	4.72	29.4	12.5	29.9	12.6	11.9
Th	7.88	9.46	10.2	1.95	29.9	18.3	29.4	7.38	6.74
U	1.96	3.32	2.84	0.51	8.71	4.18	9.34	3.32	2.41
Sc	12	13	11	21	5	26	5	2	3
V	132	126	126	181	122	343	128	7	12
Cr	28	49	23	198		0	0		
Ni	15	27	19	76	24	20	9	3	4
Cu	17	38	41	43		4	1		
Zn	71	77	70	80		55	58		
La	22.8	27.1	31.9	10.8	141	102	139	20.3	20.9
Ce	40.9	48.7	55.1	22.5	230	187	227	36.3	36.8
Pr	4.73	5.51	5.95	2.68	23.9	22.0	23.5	3.99	4.02
Nd	18.6	21.8	22.9	11.9	85.6	88.5	84.2	14.8	14.9
Sm	3.94	4.52	4.42	3.06	14.8	17.6	14.5	2.80	2.88
Eu	1.11	1.22	1.23	1.00	4.15	4.99	4.12	0.65	0.72
Gd	3.12	3.52	3.30	2.89	10.4	13.5	10.0	2.11	2.29
Tb	0.44	0.46	0.45	0.43	1.35	1.71	1.32	0.31	0.32
Dy	2.35	2.52	2.34	2.50	7.16	8.74	7.00	1.76	1.84
Ho	0.43	0.45	0.41	0.49	1.31	1.48	1.28	0.35	0.36
Er	1.08	1.13	1.05	1.21	3.33	3.59	3.26	0.94	1.01
Tm	0.15	0.15	0.15	0.17	0.49	0.48	0.48	0.14	0.15
Yb	0.88	0.92	0.86	1.01	3.02	2.73	3.01	0.94	0.99
Lu	0.15	0.15	0.14	0.16	0.47	0.40	0.46	0.15	0.17

Table 1: continued

Sample:	Sg-13	Gp-1	3D1 An†	2G3T-A†	HHV	At-02†	957 g†
Center:	Sangay	Pichincha	Antisana	Antisana	Antisana	Atacazo	Atacazo
Rock type:	dacite	dacite	andesite	andesite	andesite	andesite	andesite
SiO <sub>2</sub>	63-81	64-26	56-29	55-76	57-57	58-65	62-57
TiO <sub>2</sub>	0-49	0-39	1-04	1-06	0-91	0-66	0-62
Al <sub>2</sub> O <sub>3</sub>	17-16	16-90	15-59	18-23	16-02	16-21	16-48
FeO*	3-84	4-47	7-29	7-56	6-71	7-75	6-63
MnO	0-09	0-09	0-11	0-12	0-12	0-12	0-09
MgO	2-60	2-55	5-26	3-94	5-86	4-96	2-69
CaO	4-50	5-24	7-17	7-14	6-91	6-80	5-64
Na <sub>2</sub> O	4-26	4-19	3-72	4-18	3-58	3-84	4-10
K <sub>2</sub> O	2-98	1-78	2-99	1-68	2-10	0-87	1-06
P <sub>2</sub> O <sub>5</sub>	0-28	0-13	0-54	0-32	0-23	0-14	0-13
Rb	96-6	40-0	86-0	37-5	73-9	21-9	17-2
Sr	894	534	1245	875	594	438	355
Y	15-6	9-20	23-2	18-2	18-0	18-2	16-4
Zr	140	81	240	132	145	120	77
Nb	11-0	2-49	11-2	7-99	8-25	4-24	2-81
Cs	4-63	1-02	2-95	0-67	3-67	0-73	0-42
Ba	1054	782	1283	782	614	485	387
Hf	3-85	2-39	6-36	3-70	4-08	3-43	2-26
Ta	0-95	0-18	0-71	0-49	0-95	0-30	0-21
Pb	19-9	6-83	16-8	8-74	11-7	5-17	4-04
Th	14-3	3-06	17-1	4-89	11-9	0-99	0-18
U	6-14	1-10	4-77	1-38	4-42	0-66	0-49
Sc	9	11	19	18	20	23	26
V	85	111	183	186	165	188	135
Cr	61	33			252		
Ni	37	23	71	18	92	47	20
Cu	65	41			55		
Zn	59	61			80		
La	28-3	12-0	60-9	26-5	24-0	11-9	6-83
Ce	49-6	20-9	110	49-3	45-2	24-4	13-7
Pr	5-46	2-43	13-1	5-81	5-28	3-26	1-89
Nd	21-1	9-92	52-8	24-3	21-6	15-0	8-73
Sm	4-11	2-28	10-5	5-30	4-79	3-97	2-54
Eu	0-98	0-68	2-73	1-57	1-24	1-14	0-84
Gd	3-19	1-99	7-68	4-45	4-17	3-88	2-83
Tb	0-46	0-30	0-95	0-65	0-62	0-60	0-49
Dy	2-69	1-78	4-76	3-59	3-49	3-49	2-99
Ho	0-53	0-34	0-83	0-66	0-68	0-67	0-62
Er	1-48	0-90	2-02	1-75	1-73	1-75	1-69
Tm	0-22	0-13	0-27	0-24	0-26	0-25	0-26
Yb	1-44	0-78	1-57	1-47	1-58	1-49	1-60
Lu	0-23	0-12	0-24	0-22	0-24	0-24	0-25

Major elements, Ni, Cr, V, Cu and Zn were by measured by XRF. Others were measured by ICP-MS. Major element (wt %) compositions are reported on an anhydrous basis and normalized to 100%.

\*Total iron given as FeO.

†XRF data for Antisana (except HHV), Atacazo, and Sumaco are from Barragan *et al.* (1998).

Table 2: Whole-rock Pb, Sr, and Nd isotope compositions for Ecuador lavas

Sample	Center	Rock type	$^{206}\text{Pb}/^{204}\text{Pb}$	$^{207}\text{Pb}/^{204}\text{Pb}$	$^{208}\text{Pb}/^{204}\text{Pb}$	$^{87}\text{Sr}/^{86}\text{Sr} \pm 2\sigma$	$^{143}\text{Nd}/^{144}\text{Nd} \pm 2\sigma$	$\epsilon\text{Nd}$	$\Delta 7/4 \text{ Pb}$
3D3	Sumaco	basalt	18-872	15-602	38-660	0-704399 $\pm$ 10	0-512900 $\pm$ 10	5-17	6-50
GS5	Sumaco	bas-and	18-792	15-581	38-520	0-704140 $\pm$ 11	0-512889 $\pm$ 14	4-95	5-27
GS4	Sumaco	bas-and	18-796	15-583	38-529	0-704156 $\pm$ 10	0-512926 $\pm$ 14	5-67	5-47
lmb-1	lmbabura	andesite	19-098	15-600	38-770	0-704081 $\pm$ 10	0-512902 $\pm$ 06	5-21	3-88
lmb-3	lmbabura	andesite	19-099	15-606	38-786	0-704080 $\pm$ 08	0-512907 $\pm$ 07	5-30	4-47
lmb-11	lmbabura	andesite	19-072	15-611	38-766	0-704065 $\pm$ 08	0-512926 $\pm$ 08	5-68	5-26
lmb-26	lmbabura	andesite	18-921	15-607	38-614	0-704120 $\pm$ 11	0-512876 $\pm$ 08	4-71	6-49
lmb-28	lmbabura	andesite	18-953	15-616	38-657	0-704060 $\pm$ 10	0-512915 $\pm$ 11	5-46	7-05
lmb-29	lmbabura	andesite	18-974	15-629	38-717	0-704109 $\pm$ 10	0-512889 $\pm$ 08	4-96	8-12
lmb-30	lmbabura	andesite	18-913	15-622	38-677	0-704199 $\pm$ 11	0-512824 $\pm$ 07	3-69	8-08
lmb-36	lmbabura	andesite	19-123	15-617	38-833	0-704015 $\pm$ 11	0-512905 $\pm$ 07	5-27	5-31
lmb-38	lmbabura	andesite	18-900	15-630	38-712	0-704246 $\pm$ 08	0-512817 $\pm$ 08	3-55	9-03
lmb-45	lmbabura	andesite	19-073	15-618	38-784	0-704022 $\pm$ 10	0-512898 $\pm$ 09	5-12	5-95
Pul-9	Pululagua	andesite	18-934	15-605	38-610	0-704117 $\pm$ 10	0-512911 $\pm$ 09	5-39	6-15
Pul-11	Pululagua	andesite	18-893	15-606	38-562	0-704139 $\pm$ 11	0-512917 $\pm$ 06	5-50	6-70
Ch-3	Chacana	andesite	18-956	15-613	38-680	0-704036 $\pm$ 11	0-512841 $\pm$ 13	4-03	6-75
Ch-6	Chacana	andesite	18-983	15-633	38-755	0-704317 $\pm$ 13	0-512768 $\pm$ 08	2-59	8-41
Ch-7	Chacana	andesite	19-028	15-688	38-947	0-704234 $\pm$ 10	0-512763 $\pm$ 07	2-49	13-45
3D1 An	Antisana	andesite	18-936	15-618	38-728	0-704144 $\pm$ 11	0-512845 $\pm$ 11	4-09	7-48
2G3T-A	Antisana	andesite	18-924	15-643	38-762	0-704374 $\pm$ 10	0-512751 $\pm$ 08	2-27	10-05
HHV	Antisana	andesite	18-985	15-703	38-978	0-704163 $\pm$ 13	0-512793 $\pm$ 07	3-08	15-42
At-02	Atacazo	andesite	18-933	15-602	38-619	0-704084 $\pm$ 11	0-512893 $\pm$ 07	5-04	5-83
957 g	Atacazo	andesite				0-704301 $\pm$ 11	0-512878 $\pm$ 13	4-73	
ll-2	llalo	andesite				0-704059 $\pm$ 10	0-512859 $\pm$ 08	4-36	
Pul-4	Pululagua	dacite	18-921	15-595	38-572	0-704139 $\pm$ 10	0-512954 $\pm$ 23	6-22	5-29
Pul-7	Pululagua	dacite	18-921	15-596	38-572	0-704139 $\pm$ 10	0-512894 $\pm$ 24	5-06	5-39
Ql-12	Quilotoa	dacite	18-985	15-644	38-750	0-704033 $\pm$ 11	0-512861 $\pm$ 08	4-41	9-50
Ch-8	Chacana	dacite	18-925	15-646	38-694	0-704269 $\pm$ 11	0-512804 $\pm$ 57	3-30	10-32
Sg-13	Sangay	dacite	18-816	15-644	38-754	0-704368 $\pm$ 11	0-512739 $\pm$ 21	2-02	11-39
Gp-1	Pichincha	dacite	18-958	15-597	38-698	0-703947 $\pm$ 11	0-512888 $\pm$ 19	4-94	5-04
Cl-11	Chalupas	rhyolite	18-993	15-668	38-873	0-704432 $\pm$ 13	0-512737 $\pm$ 08	2-00	11-77
Ch-4	Chacana	rhyolite	18-925	15-646	38-775		0-512710 $\pm$ 13	1-46	10-33
Ch-5	Chacana	rhyolite	18-918	15-632	38-732	0-704337 $\pm$ 11	0-512776 $\pm$ 11	2-74	9-04
Cx-9	Cotopaxi	rhyolite	18-963	15-631	38-710	0-704135 $\pm$ 10	0-512823 $\pm$ 09	3-67	8-41
Cx-10	Cotopaxi	rhyolite	18-951	15-637	38-716	0-704187 $\pm$ 10	0-512839 $\pm$ 09	3-98	9-22

## RESULTS

### Basalts and basaltic andesites (Sumaco Volcano)

Basalts and basaltic andesites are rare in the northern Andes, occurring in significant numbers only at Sumaco Volcano (43–54 wt %  $\text{SiO}_2$ , Table 1, Fig. 3), located in the back-arc of Ecuador (Fig. 2) ~400 km from the trench (Beate *et al.*, 2001; Bourdon *et al.*, 2003). Sumaco lavas are shoshonitic (1.05–4.12 wt %  $\text{K}_2\text{O}$ , Fig. 3) and silica-undersaturated (Pichler *et al.*, 1976). They have high

abundances of moderately compatible/incompatible elements (e.g. Y >37 ppm, Yb >2.7 ppm, Sr >2500 ppm) and concentrations of highly incompatible elements (e.g. Rb >97, Ba >1400, Ce >180,) that commonly lie well above those of normal subduction-related lavas (Fig. 4; see also Barragan *et al.*, 1998; Bourdon *et al.*, 2003). Basalts and basaltic andesites from Sumaco have strongly fractionated rare-earth element (REE) patterns ( $\text{La}/\text{Yb} = 31\text{--}43$ , Fig. 5a) and high Sr/Y despite the fact that Y and heavy REE (HREE) concentrations are also high (Fig. 6a). Concentrations of high field strength elements (HFSE)

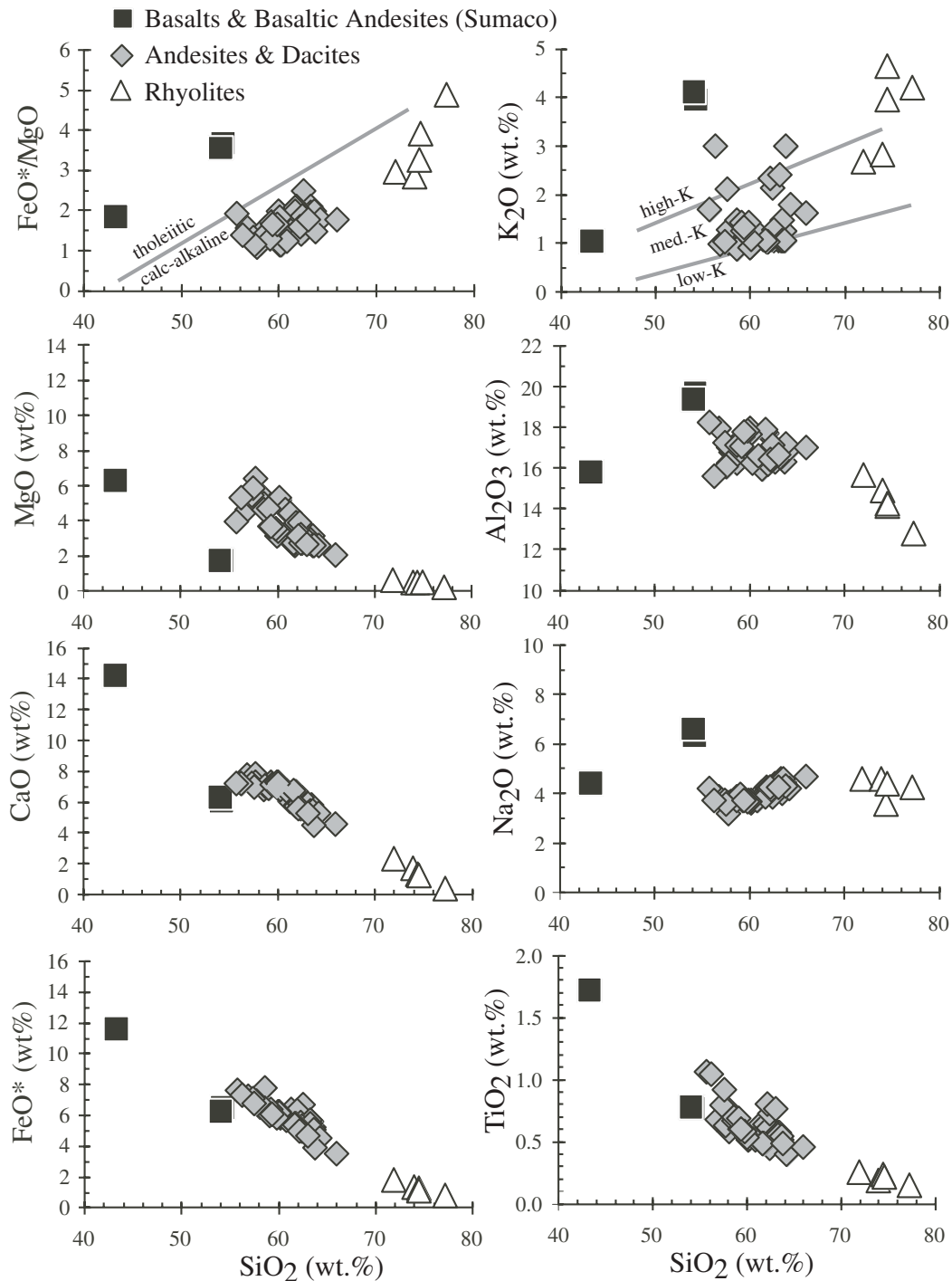


**Fig. 3.** Major element variation in Holocene–Late Pleistocene volcanic rocks from Ecuador. Data are from Table 1. Symbols for compositional categories defined here (basalt–basaltic andesite, andesite–dacite, rhyolite) are used throughout this paper. The calc-alkaline–tholeiitic boundary line is from Miyashiro (1974). Boundaries defining low-, medium- and high-K series are from Ewart (1982).

are high in an absolute sense ( $\text{Nb} > 35$  ppm, Fig. 4), but are sometimes low compared with similarly incompatible large ion lithophile elements (LILE). This is illustrated in ratios such as  $\text{Rb}/\text{Ta}$  and  $\text{Pb}/\text{Ce}$ , which are higher than

for mid-ocean ridge basalt (MORB) at Sumaco but not as high as typical arc lavas (Fig. 7). These incompatible element ratios appear to indicate that Sumaco lavas contain a subduction-related geochemical component that is

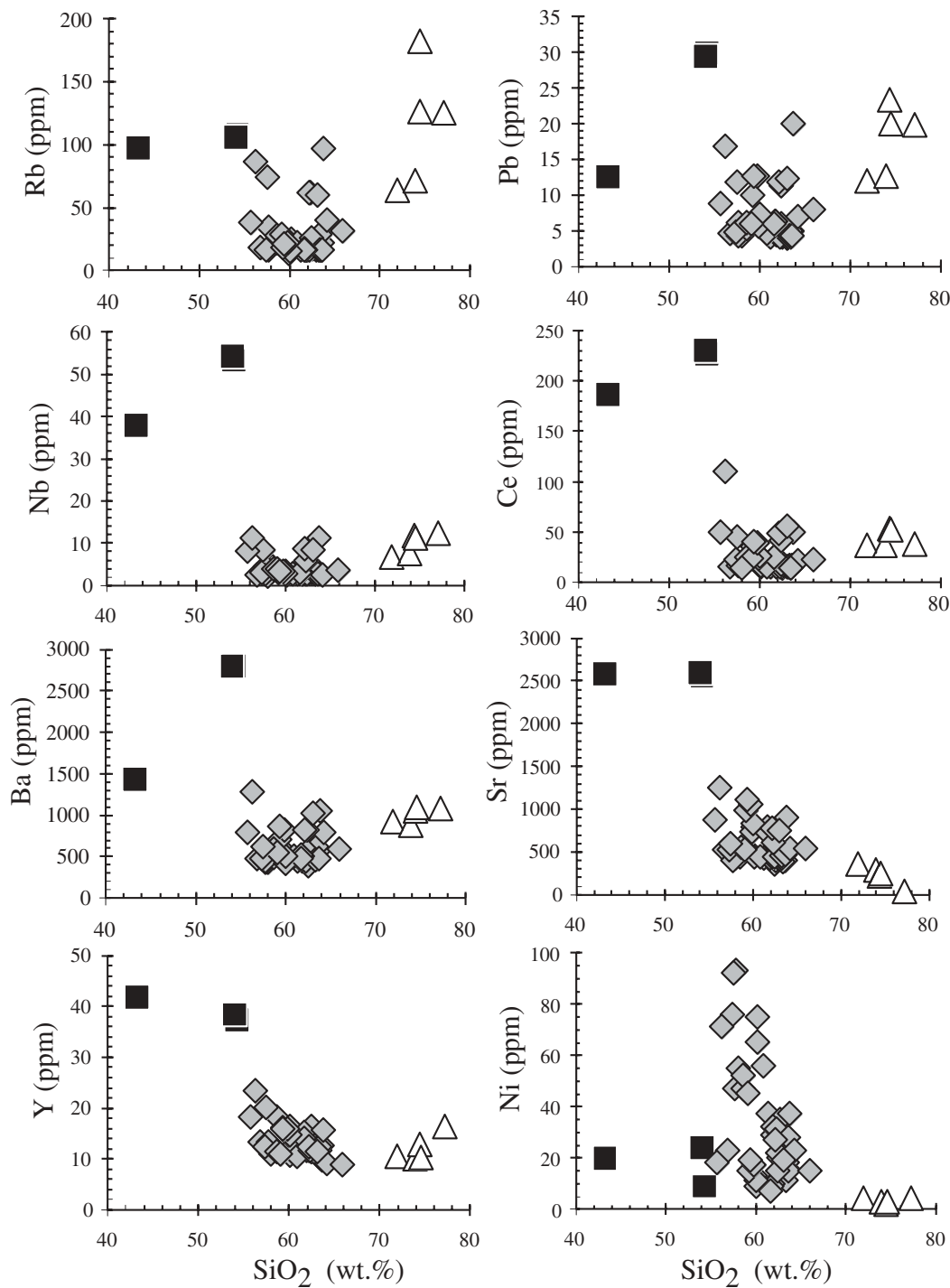


**Fig. 4.** Variation in trace element (Rb, Nb, Ba, Y, Pb, Ce, Sr, Ni) concentrations as a function of  $\text{SiO}_2$  for Ecuador volcanic rocks. All data are from Table 1. Symbols are as in Fig. 3.

slightly smaller than that present in the andesites and dacites that typify volcanism throughout Ecuador (Fig. 7; see also Barragan *et al.*, 1998, fig. 4).

Based on the above it is clear that the lavas from Sumaco are readily distinguished from all others

in Ecuador with respect to major and trace elements (Figs 3–7). In contrast, the isotopic compositions of the Sumaco samples fall generally within the relatively narrow range of compositions observed in Ecuador (e.g. Harmon *et al.*, 1984; Kilian *et al.*, 1994, 1995; Barragan

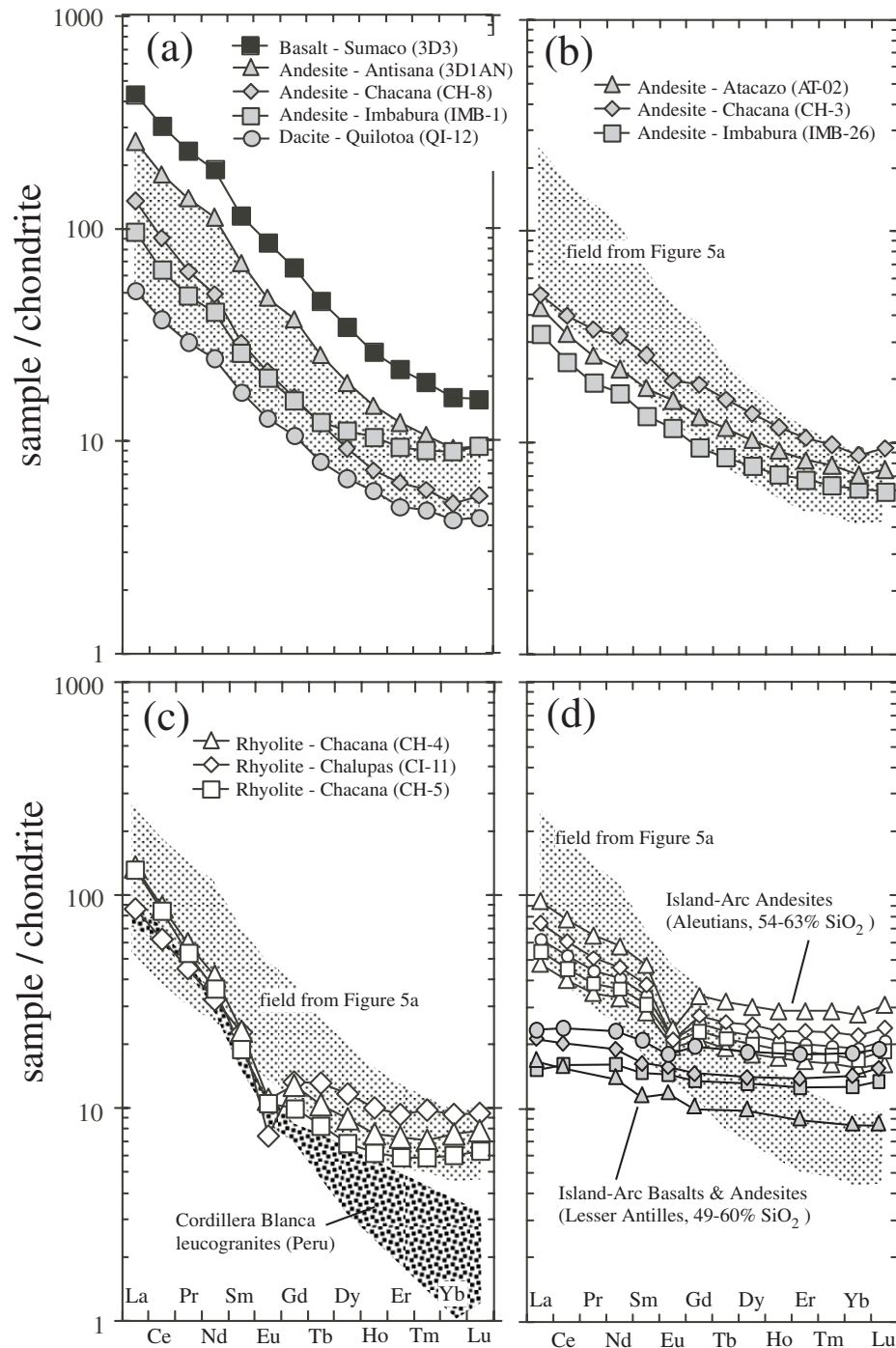


**Fig. 5.** Chondrite-normalized REE patterns of volcanic rocks from Ecuador (a, b) compared with leucogranites of the Cordillera Blanca, Peru (c) and common island arc lavas from the central Aleutian and Lesser Antilles island arcs (d). Stippled field in (b) and (c) is the field bounded by the Antisana andesite and the Quilotoa dacite in (a). Leucogranite data are from Atherton & Petford (1993). Island arc data are from Davidson (1987) and Kelemen *et al.* (2003). All other Ecuadorian data are from Table 1.

*et al.*, 1998; Bourdon *et al.*, 2003). The three samples from Sumaco that we have measured have isotope ratios for both Sr ( $^{87}\text{Sr}/^{86}\text{Sr} = 0.7041\text{--}0.7044$ ) and Nd ( $^{143}\text{Nd}/^{144}\text{Nd} = 0.51289\text{--}0.51293$ ) that fall near the

middle-to-high end of the range of values that we report for lavas of all compositions ( $^{87}\text{Sr}/^{86}\text{Sr} = 0.7040\text{--}0.7045$ ;  $^{143}\text{Nd}/^{144}\text{Nd} = 0.51273\text{--}0.51295$ ; Table 2 and Fig. 8). In contrast, the Pb isotope compositions of Sumaco lavas are

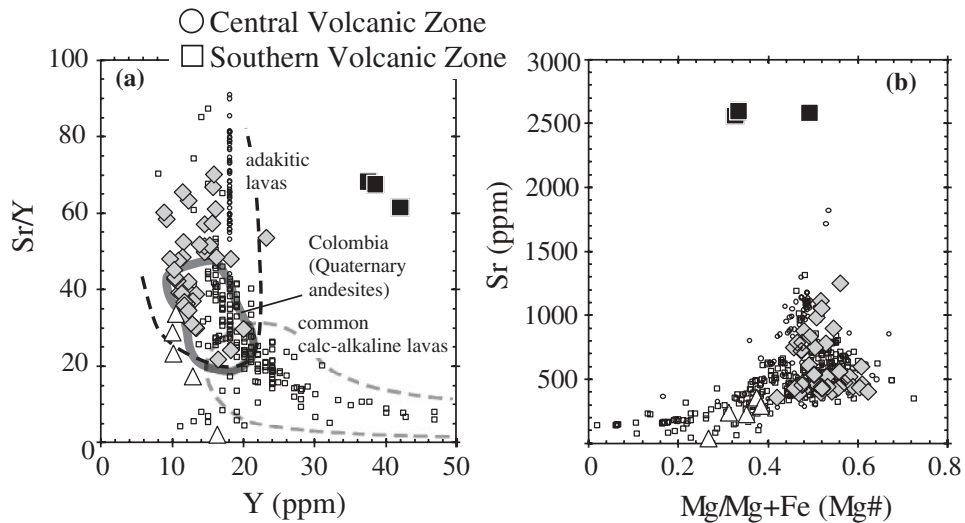


**Fig. 6.** Variation of Sr/Y vs Y (a) and Sr concentration vs Mg/(Mg + Fe) (b). Ecuadoran data (large symbols as in Fig. 3) are from Table 1. Boundaries for 'adakitic' and 'common calc-alkaline' fields have been approximated from Defant *et al.* (1991, fig. 15). Central and Southern Andean volcanic zone data are from published sources (Lopez-Escobar *et al.*, 1977, 1985; Deruelle, 1982; Thorpe *et al.*, 1983; Frey *et al.*, 1984; Harmon *et al.*, 1984; Lopez-Escobar, 1984; Hickey *et al.*, 1986; Davidson *et al.*, 1988, 1990; Futa & Stern, 1988; Gerlach *et al.*, 1988; Hildreth & Moorbath, 1988; Wörner, 1989; Walker *et al.*, 1991). Field for Quaternary andesites in Colombia is from Sigurdsson *et al.* (1990), Droux & Delaloye (1996) and Calvache & Williams (1997).

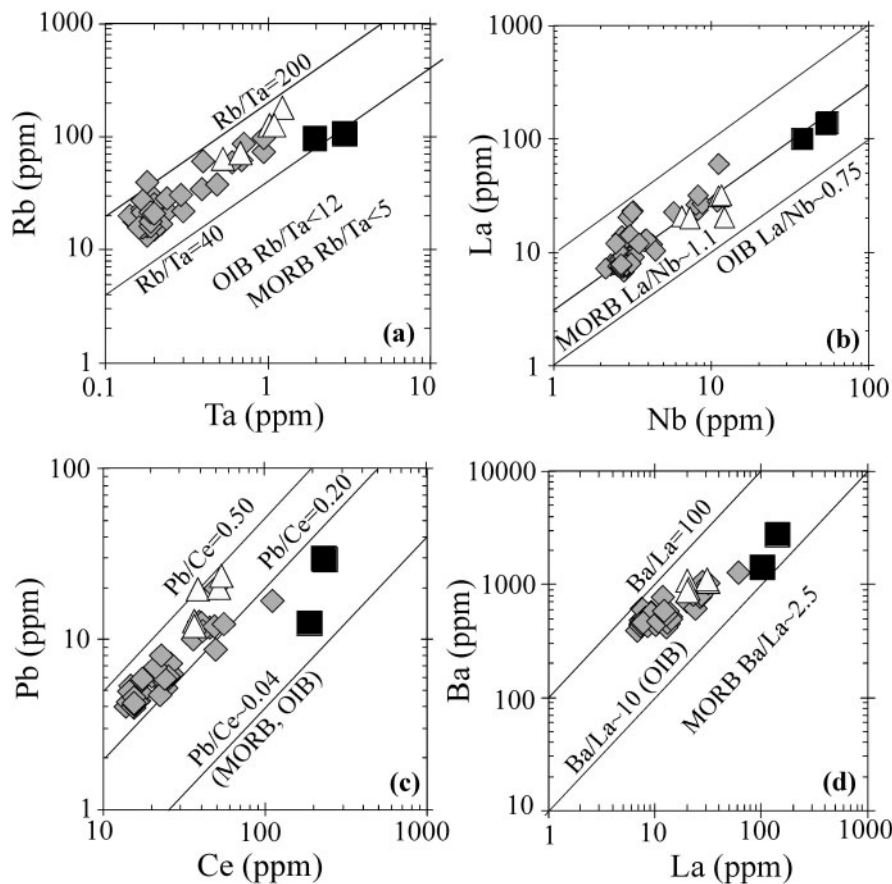


**Fig. 7.** Incompatible element concentrations and ratios in Ecuadoran lavas compared with average values for MORB and OIB: (a) Rb-Ta; (b) La-Nb; (c) Pb-Ce; (d) Ba-La. Ecuadoran data are from Table 1. Symbols used here are as in Fig. 3. Values for MORB and OIB are from Sun & McDonough (1989).

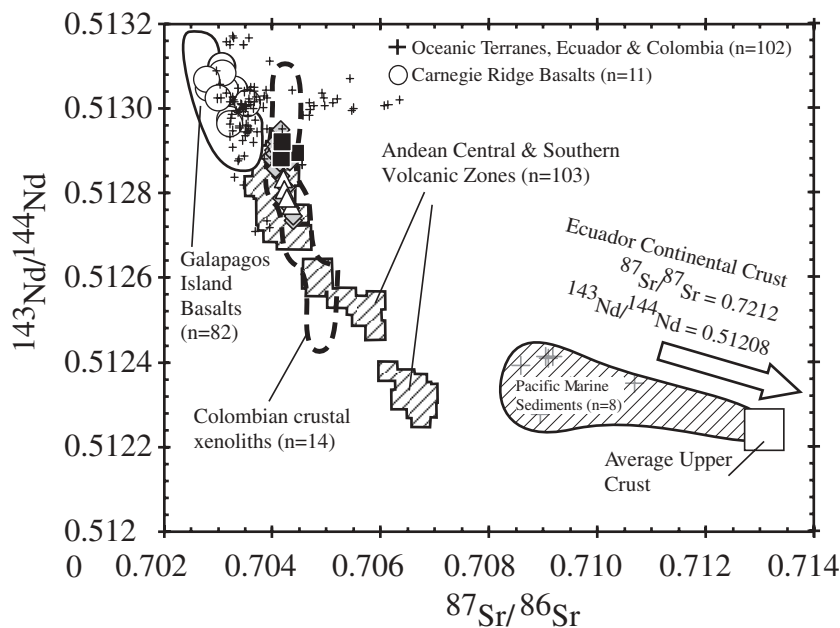


**Fig. 8.** Variation in  $^{143}\text{Nd}/^{144}\text{Nd}$  vs  $^{87}\text{Sr}/^{86}\text{Sr}$  showing the compositions of lavas from Ecuador compared with data from the Galapagos plume and Carnegie Ridge (White *et al.*, 1993; Hauff *et al.*, 1999; Harpp & White, 2001; Werner *et al.*, 2003), the Andean Central and Southern Volcanic Zones (Frey *et al.*, 1984; Hickey *et al.*, 1986; Davidson *et al.*, 1988, 1990; Futa & Stern, 1988; Hildreth & Moorbath, 1988; Wörner, 1989; Walker *et al.*, 1991), Pacific pelagic sediments (Ben Othman *et al.*, 1989), average upper crust (Zartman & Haines, 1988), Mesozoic oceanic terranes in Colombia and Ecuador (Kerr *et al.*, 1996, 1997, 2002, 2004; Reynaud *et al.*, 1999; Hauff *et al.*, 2000; Lapierre *et al.*, 2000; Mamberti *et al.*, 2003) and continental crust in Ecuador (Bosch *et al.*, 2002). Ecuadoran data are from Table 2. Symbols are as in Fig. 3.

relatively unradiogenic ( $^{206}\text{Pb}/^{204}\text{Pb} = 18.792\text{--}18.872$ ;  $^{207}\text{Pb}/^{204}\text{Pb} = 15.581\text{--}15.602$ ) and fall within the field of Galapagos basalts, and at the low end of a nearly vertical array of Ecuador data on plots of  $^{207}\text{Pb}/^{204}\text{Pb}$  vs  $^{206}\text{Pb}/^{204}\text{Pb}$ , that spans the compositional range from the Galapagos Plume to average upper crust and/or local basement rocks in Ecuador (Fig. 9).

### Andesites and dacites

Medium-K, calc-alkaline andesites and dacites ( $\text{SiO}_2 = 55.76\text{--}65.98\%$ ,  $\text{FeO}^*/\text{MgO} = 1.39\text{--}1.76$ ) are the predominant magma types erupted in Ecuador (Table 1, Fig. 3). Major element contents of MgO (2.00–6.40 wt %), CaO (4.53–7.80 wt %), FeO\* (3.51–7.75 wt %) and  $\text{Na}_2\text{O}$  (3.18–4.68 wt %) all show coherent linear trends when plotted against  $\text{SiO}_2$  (Fig. 3). In contrast,  $\text{K}_2\text{O}$  (0.87–2.99 wt %) varies two-fold across the andesite–dacite compositional range and is not correlated with increasing  $\text{SiO}_2$  (Fig. 3).

Highly incompatible trace elements in the andesites and dacites (Rb, Ba, Ta, Nb, La, etc.) are generally correlated with one another (Fig. 7), but like  $\text{K}_2\text{O}$ , are not well correlated with major element differentiation indicators such as  $\text{SiO}_2$  or MgO (e.g. Fig. 4). Strontium (Sr) and Y, which typically exhibit moderately incompatible behavior in subduction-related lavas, are highly

variable in abundance (Sr = 450–1200 ppm; Y = 9–23 ppm), but show no clear relationship when plotted against strongly incompatible elements such as Cs, Rb or Ba. Strontium is similarly uncorrelated with  $\text{SiO}_2$  but does decrease systematically with decreasing Mg-number [ $\text{Mg}/(\text{Mg} + \text{Fe})$ , Fig. 6b]. Yttrium (Y), which is relatively low in abundance in most samples (commonly <15 ppm), generally decreases with increasing  $\text{SiO}_2$  between 56% and 64%  $\text{SiO}_2$ , indicating that it has behaved as a moderately compatible element during the evolution of these lavas (see also Monzier *et al.*, 1999, fig. 11). Abundances of strongly compatible trace elements, such as Cr and Ni, are highly variable in the andesites and dacites (Cr up to 240 ppm), and like many of the most incompatible elements, also appear to be largely independent of  $\text{SiO}_2$  (e.g. Fig. 4).

Ratios among the incompatible elements in the andesites and dacites are clearly characteristic of a subduction zone setting, and in most respects are typical of andesites and dacites throughout the Andes. Ratios of LILE to HFSE (e.g. Rb/Ta, Ba/Nb) are elevated in the andesites and dacites compared with oceanic basalts (Fig. 7). The REE are highly variable with regard to both elemental abundance and pattern shape (Fig. 5). The total range for La/Yb is high (4.3–38.8; Fig. 10, Table 1), but there is a strong clustering of samples at relatively low La/Yb (6–10) with a few more highly



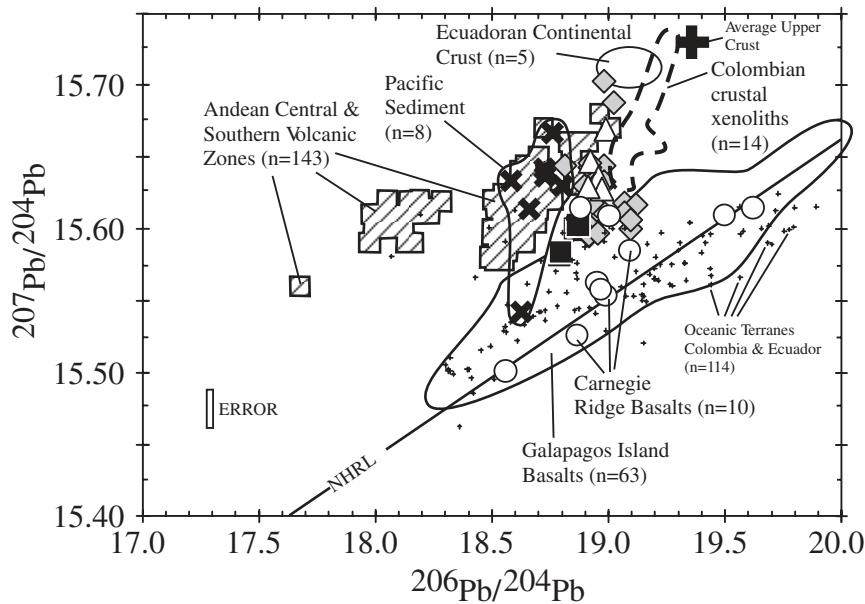


**Fig. 9.** Variation in  $^{207}\text{Pb}/^{204}\text{Pb}$  vs  $^{206}\text{Pb}/^{204}\text{Pb}$  showing the compositions of lavas from Ecuador compared with data from the Galapagos plume and Carnegie Ridge (White *et al.*, 1993; Hauff *et al.*, 1999; Harpp & White, 2001; Werner *et al.*, 2003), the Andean Central and Southern Volcanic Zones (Hickey *et al.*, 1986; Davidson *et al.*, 1988, 1990; Hildreth & Moor bath, 1988; Wörner, 1989), average upper crust (Zartman & Haines, 1988), Mesozoic oceanic terranes in Colombia and Ecuador (Dupré & Echeverría, 1984; Zartman & Haines, 1988; Kerr *et al.*, 1996, 1997, 2002, 2004; Reynaud *et al.*, 1999; Hauff *et al.*, 2000; Lapierre *et al.*, 2000; Mamberti *et al.*, 2003) and continental crust in Ecuador (Bosch *et al.*, 2002). Northern Hemisphere Reference Line (NHRL) is from Hart (1984). Ecuador data are from Table 2. Symbols are as in Fig. 3.

fractionated samples (only four samples with  $\text{La}/\text{Yb} > 20$ ; Fig. 10). Among the samples with  $\text{La}/\text{Yb} > 10$ , some are clearly depleted in the HREE ( $\text{Yb} < 1.0$ ) and have fractionated HREE patterns with normalized  $\text{Dy}/\text{Yb} > 2.0$ , whereas others are primarily enriched in the light REE (LREE) and have flatter HREE patterns (Fig. 5a). The most common andesites and dacites have straight and modestly fractionated patterns with  $\text{La}/\text{Yb} = 6\text{--}10$  and normalized  $\text{Dy}/\text{Yb} < 2.0$  (Fig. 5b). Overall, these REE characteristics do not stand out as unusual compared with andesites and dacites from other parts of the Andes (Fig. 10). Barium (Ba) concentrations are also variable, and  $\text{Ba}/\text{La}$  ratios are relatively high in the andesites and dacites ( $\text{Ba}/\text{La} = 20\text{--}80$ ); in this respect the Ecuadoran lavas are similar to lavas in island arcs but are unlike andesites and dacites of the central and southern Andes, which typically have  $\text{Ba}/\text{La} < 25$  (Fig. 10; Hildreth & Moor bath, 1988; Davidson *et al.*, 1990). In addition, nearly all of the andesites and dacites from Ecuador have high  $\text{Sr}/\text{Y}$  (22–70; Figs 6a and 10), and according to the criteria of Defant & Drummond (1990) most would be classified as adakites (see also Beate *et al.*, 2001; Bourdon *et al.*, 2002, 2003; Samaniego *et al.*, 2002). In this regard again, the rocks from Ecuador are also typical of andesites and dacites from throughout the Andes (Figs 6 and 10).

Trace element characteristics in the andesites and dacites also change systematically from west to east across

the magmatic arc in Ecuador. In general, the average incompatible element concentrations are higher in the main arc and back-arc areas, at greater distances from the trench (Fig. 11a and b). Certain incompatible-element ratios (e.g.  $\text{Ba}/\text{Nb}$  and  $\text{La}/\text{Yb}$ ) also change systematically across the arc (Fig. 11c and d; see also Hörmann & Pichler, 1982; Kilian & Pichler, 1989; Vanek *et al.*, 1994; Barragan *et al.*, 1998). These patterns are similar to those seen in magmatic arcs worldwide (Dickinson, 1975).

Isotopically, the andesites and dacites from Ecuador define a relatively narrow range of values that fall within the Sr–Nd mantle array and overlap somewhat with Galapagos plume basalts for each of the isotopic systems studied (Sr, Nd, Pb; Figs 8 and 9). Isotope ratios for Sr and Nd ( $^{87}\text{Sr}/^{86}\text{Sr} = 0.7040\text{--}0.7044$ ,  $^{143}\text{Nd}/^{144}\text{Nd} = 0.51273\text{--}0.51295$ ; Table 2) lie at the high  $^{143}\text{Nd}/^{144}\text{Nd}$  end of the field of modern Andean lavas (Fig. 8), and encompass nearly the full range of published values for the Northern Volcanic Zone (Harmon *et al.*, 1984; Kilian *et al.*, 1995; Barragan *et al.*, 1998; Bourdon *et al.*, 2003). For Pb isotopes, the andesites and dacites form a near-vertical trend on plots of  $^{207}\text{Pb}/^{204}\text{Pb}$  vs  $^{206}\text{Pb}/^{204}\text{Pb}$ , spanning the compositional gap between Galapagos basalts and average upper crust and/or local basement (Fig. 9). The data from Ecuador are broadly like those from Colombia (James & Murcia, 1984), but contrast sharply with the Pb isotope compositions of lavas

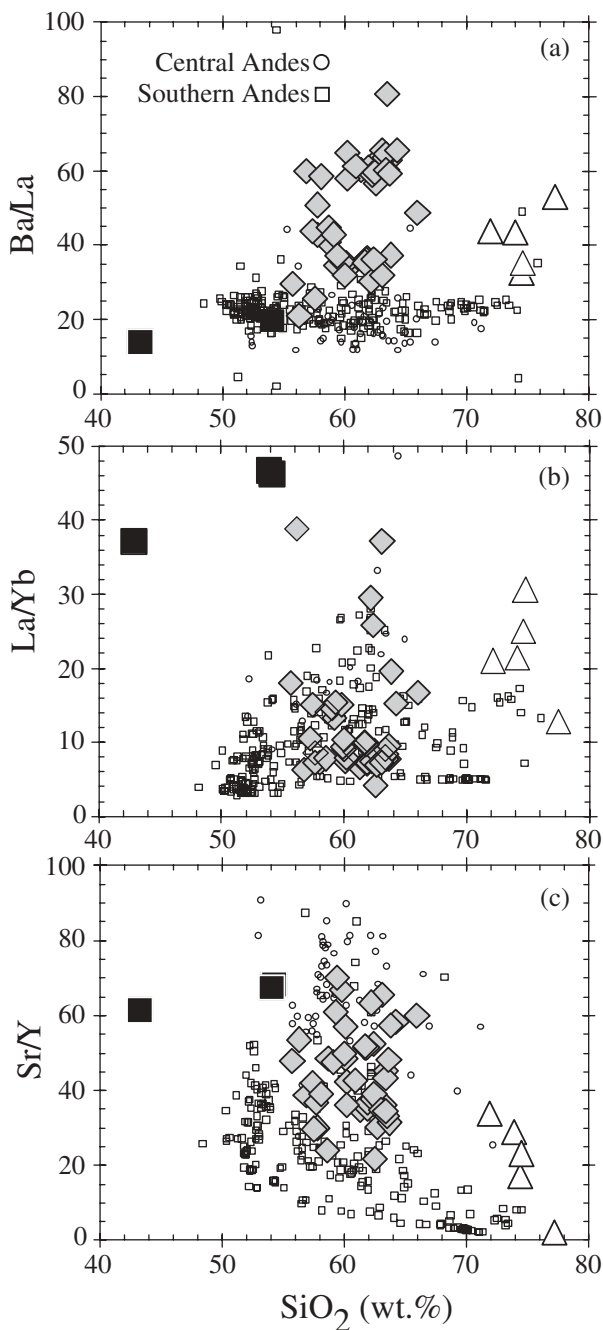


**Fig. 10.** Ba/La (a), La/Yb (b) and Sr/Y (c) vs SiO<sub>2</sub> (wt %) comparing lavas from Ecuador with those from the Andean Central and Southern Volcanic Zones. Ecuador data are from Table 1. Symbols are as in Fig. 3. Published data sources for the central and southern Andes are listed in the captions to Figs 6, 8 and 9.

from the central and southern Andes, which commonly have <sup>206</sup>Pb/<sup>204</sup>Pb values that are relatively low, but <sup>207</sup>Pb/<sup>204</sup>Pb values that are high, resulting in a nearly horizontal data array in <sup>207</sup>Pb/<sup>204</sup>Pb vs <sup>206</sup>Pb/<sup>204</sup>Pb (Fig. 9). It is useful to quantify the Pb isotope variation

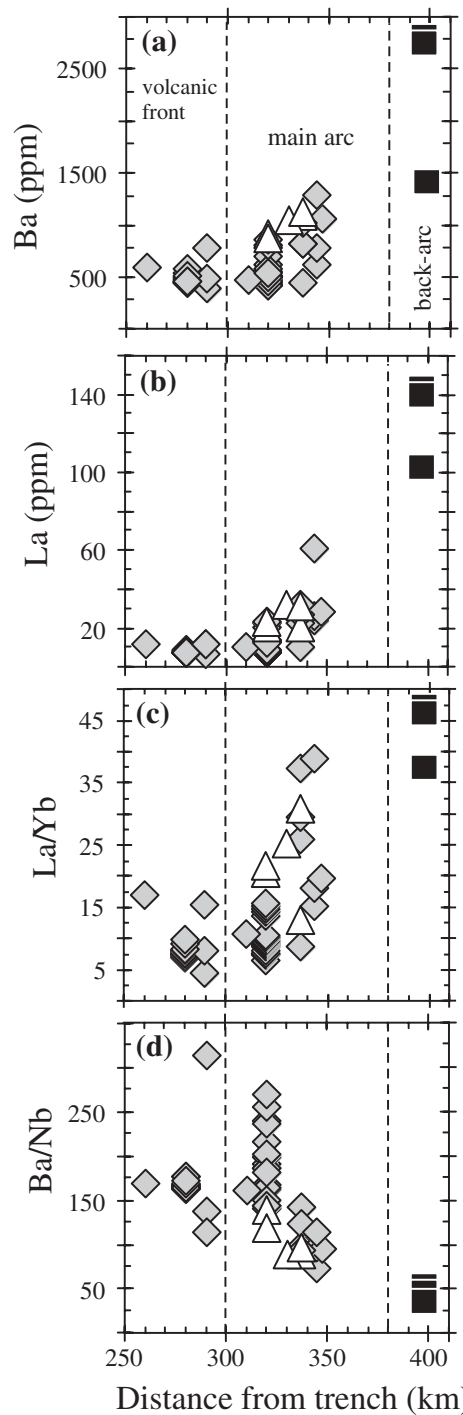


**Fig. 11.** Trace element concentrations for (a) Ba and (b) La, and ratios (c) La/Yb and (d) Ba/Nb plotted against distance from trench across Ecuador. Data are from Table 1.

in Andean lavas in terms of the parameter  $\Delta 7/4$  Pb, which is a quantitative expression of the deviation in <sup>207</sup>Pb/<sup>204</sup>Pb from the mantle reference line at the <sup>206</sup>Pb/<sup>204</sup>Pb composition of the sample (Hart, 1984).

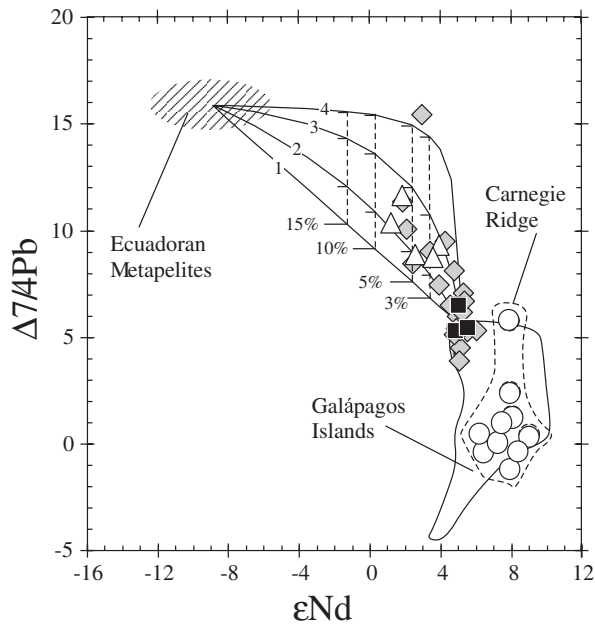


**Fig. 12.** Variation of  $\Delta 7/4\text{Pb}$  vs  $\epsilon\text{Nd}$  for Ecuador lavas. Bulk mixing lines (labeled 1–4) are between estimated Ecuador basalt (3 ppm Pb, 5 ppm Nd,  $^{143}\text{Nd}/^{144}\text{Nd} = 0.512900$ ,  $\epsilon\text{Nd} = 5.11$ ,  $^{207}\text{Pb}/^{204}\text{Pb} = 15.589$ ,  $^{206}\text{Pb}/^{204}\text{Pb} = 18.820$ ) and putative crustal assimilants with isotopic compositions like those of Ecuador metapelites ( $^{143}\text{Nd}/^{144}\text{Nd} = 0.512183$ ,  $\epsilon\text{Nd} = -8.9$ ,  $^{207}\text{Pb}/^{204}\text{Pb} = 15.700$  and  $^{206}\text{Pb}/^{204}\text{Pb} = 18.916$ ). The isotopic composition of the metapelite end-member is from Bosch *et al.* (2002). Mixing line 1 uses the Pb and Nd concentrations of the average metapelites (Nd = 25 ppm, Pb = 15 ppm). Subsequent mixing lines use higher Pb concentrations for the assimilant (higher Pb/Nd in the metapelite end-member) to produce the curved mixing lines, which bracket the Ecuadoran lavas (Pb/Nd = 1.2 and 4.0). The isotopic composition for the basalt end-member is the average of the Sumaco lavas (Table 2), which appear to be relatively unaffected by assimilation. Concentrations for Nd and Pb in the basalt end-member were estimated by extrapolating andesite compositions for these elements back to  $\sim 52\%$   $\text{SiO}_2$  (on graphs of Nd and Pb vs  $\text{SiO}_2$ ). Values for  $\Delta 7/4\text{Pb}$  were calculated according to Hart (1984). Sources of published data from the Carnegie Ridge and Galapagos Islands are as in Figs 8 and 9.

Expressed in this way, Pb isotope compositions in Ecuador andesites and dacites show a crude inverse correlation with Nd isotopes, and appear to fall along mixing lines between Galapagos plume basalts and pelitic metasediments from the local continental crust (Fig. 12).

The isotopic compositions of the andesites and dacites change both east-to-west across the magmatic arc in Ecuador, and with changes in certain trace element parameters. Specifically,  $^{87}\text{Sr}/^{86}\text{Sr}$  and  $\Delta 7/4\text{Pb}$  in the Ecuadoran lavas reach their highest values in lavas erupted in the main-arc region (330–360 km from the trench), along the crest of the Andes, where the crust is likely to be thickest (Fig. 13). Conversely,  $^{143}\text{Nd}/^{144}\text{Nd}$  ( $\epsilon\text{Nd}$ ) is lowest across this region. It should be noted, however, that the alkali basalts and basaltic andesites from Sumaco Volcano in the back-arc area do not follow the cross-arc

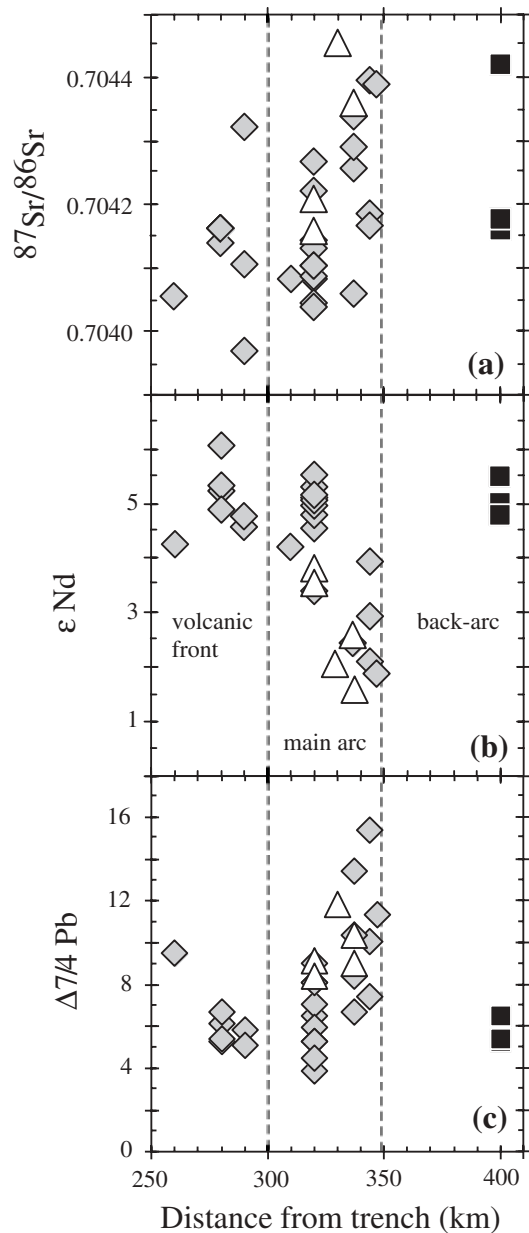


**Fig. 13.** Isotope ratios plotted against distance from trench across Ecuador, showing cross-arc changes in  $^{87}\text{Sr}/^{86}\text{Sr}$  (a),  $\epsilon\text{Nd}$  (b), and  $\Delta 7/4\text{Pb}$  (c) in lavas produced at different positions across the arc. Data plotted here are from Table 2. Symbols used here are as in Fig. 3.

isotopic trends of the andesites and dacites (Fig. 13). The isotopic compositions of the andesites and dacites in Ecuador also change systematically with increasing incompatible element concentrations (e.g. decreasing  $^{143}\text{Nd}/^{144}\text{Nd}$  with increasing Nb, Ba, Rb, La; Fig. 14), and with changes in certain trace element ratios, especially Ba/Nb and La/Yb, and to a lesser extent Ba/La (Fig. 15). In general, the trace element–isotope relationships are clearest for Nd and Pb isotopes, but are absent

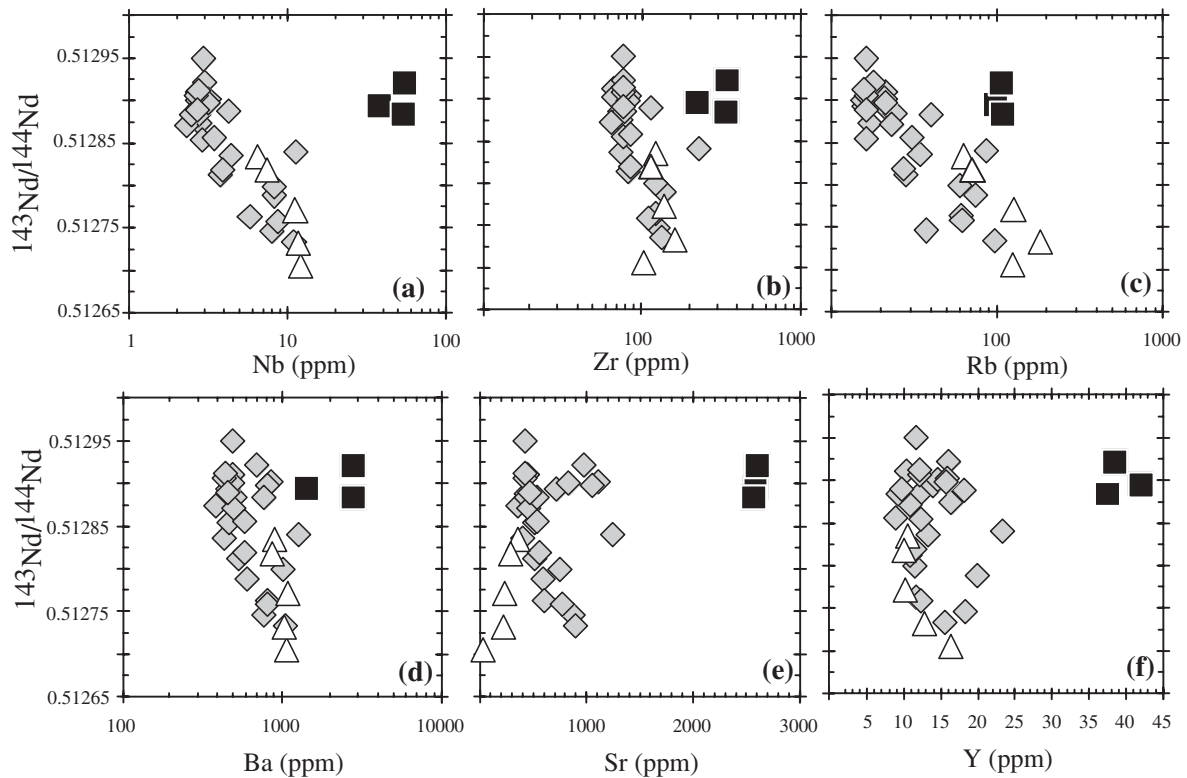


**Fig. 14.**  $^{143}\text{Nd}/^{144}\text{Nd}$  vs Nb (a), Zr (b), Rb, (c), Ba (d), Sr (e) and Y (f) in Ecuadoran lavas. Data are from Tables 1 and 2. Symbols are as in Fig. 3.

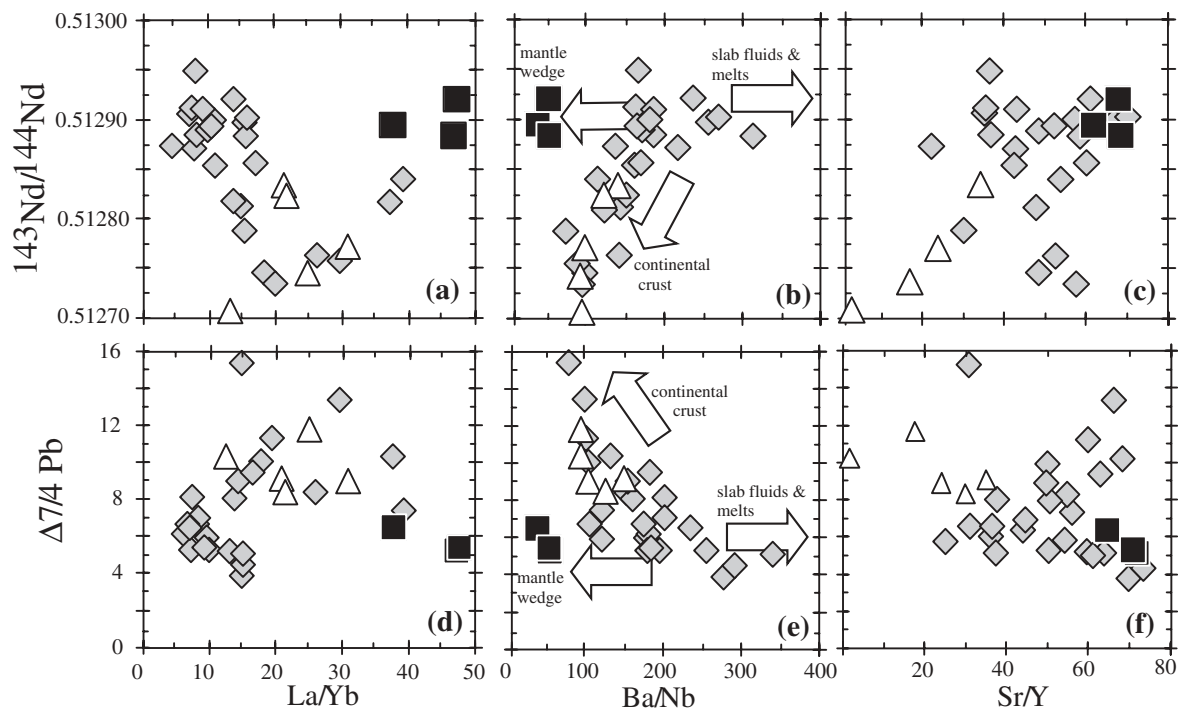


**Fig. 15.**  $^{143}\text{Nd}/^{144}\text{Nd}$  and  $\Delta 7/4\text{Pb}$  vs La/Yb (a, d), Ba/Nb (b, e) and Sr/Y (c, f) for Ecuadoran lavas. Large white arrows on Ba/Nb plots provide an interpretation of source components in the mantle wedge (low  $\Delta 7/4\text{Pb}$  and Ba/Nb; high  $^{143}\text{Nd}/^{144}\text{Nd}$ ), fluids and/or melts from the subducting oceanic crust (low  $\Delta 7/4\text{Pb}$ ; high Ba/Nb and  $^{143}\text{Nd}/^{144}\text{Nd}$ ) and continental crust (high  $\Delta 7/4\text{Pb}$ ; low Ba/Nb and  $^{143}\text{Nd}/^{144}\text{Nd}$ ). Data are from Tables 1 and 2. Symbols are as in Fig. 3.

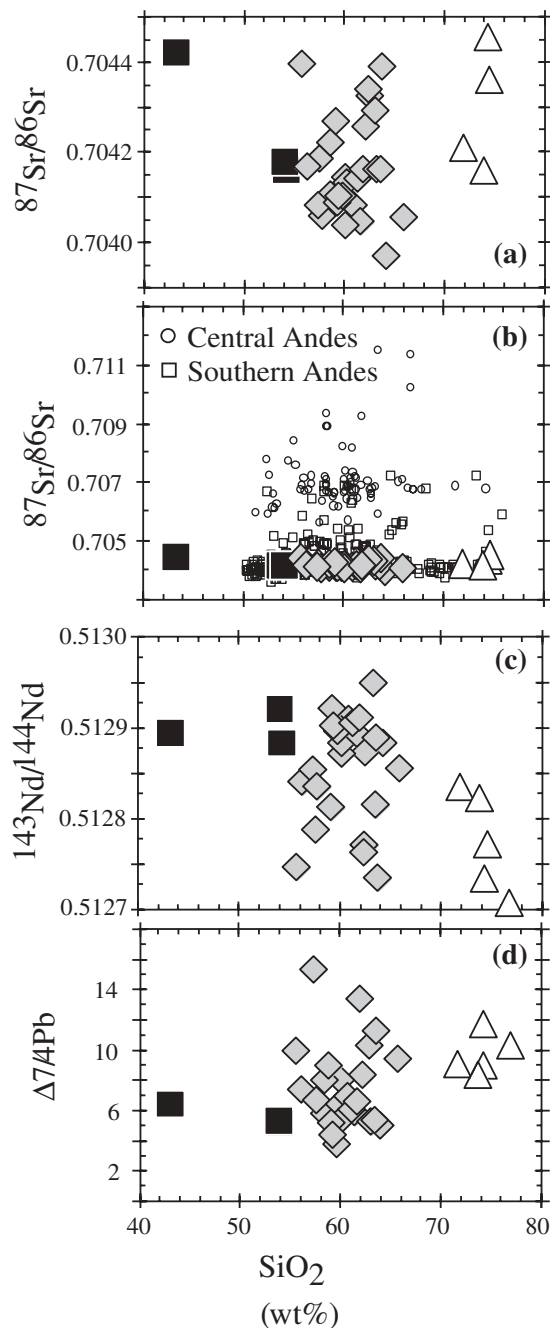


**Fig. 16.** Variation in  $^{87}\text{Sr}/^{86}\text{Sr}$  (a, b),  $^{143}\text{Nd}/^{144}\text{Nd}$  (c) and  $\Delta 7/4\text{Pb}$  (d) vs  $\text{SiO}_2$  for Ecuadoran lavas (large symbols), and other areas within the Andes (small symbols). Ecuadoran data are from Tables 1 and 2. Sources for other Andean data are cited in the caption to Fig. 8.

or less clear when they involve either Sr or  $^{87}\text{Sr}/^{86}\text{Sr}$ . Finally, there appears to be no clear systematic relationship between any of the isotopic systems and any major element parameter (e.g.  $\text{SiO}_2$ ) in the andesite–dacite compositional range (Fig. 16).

## Rhyolites

Rhyolites reported here are from Chacana, Chalupas, and Cotopaxi volcanoes, which are all located in the main-arc area, along the crest of the Andes in northern Ecuador (Table 1, Figs 1 and 2). Apart from the obvious gap in silica between approximately 66% and 71%  $\text{SiO}_2$  (Fig. 3), the major and trace element compositions of the rhyolites from Ecuador appear, in a broad sense, to be extensions of the andesite–dacite compositional trends (Figs 3–5). One exception is in the REE patterns, which are clearly much flatter in the HREE (normalized  $\text{Dy}/\text{Yb} < 1.50$ ) and have 18–57% negative Eu anomalies (i.e.  $\text{Eu}/\text{Eu}^* = 0.43\text{--}0.82$ ; Fig. 5c). The broad similarity with respect to trace elements does not extend to the isotopic compositions, which on average, are more radiogenic in Pb and Sr and less radiogenic in Nd in the rhyolites than in the andesites and dacites (Figs 8, 9 and 13–15). This is to be expected in high- $\text{SiO}_2$  melts containing a relatively high proportion of geochemically evolved crustal rock relative to mantle components.

## DISCUSSION

### Isotopic constraints on crustal components in Ecuadoran lavas

Compared with the central and southern Andes, where the case for substantial melting and assimilation of geochemically evolved crustal rocks has been well documented (e.g. Hildreth & Moorbath, 1988; Davidson *et al.*, 1990; Kay & Kay, 1991), lavas in Ecuador fall within a narrow range of relatively primitive isotopic compositions, partially overlapping the range of Galapagos Plume basalts for Pb and Nd isotopes (Figs 8 and 9). The isotopic compositions in Ecuadoran lavas also appear to be largely independent of their major element compositions (Fig. 16) and of the age or composition of the crust through which they were erupted (e.g. compare back-arc and volcanic front in Fig. 13). This is particularly evident for the lavas from Sumaco, which are mafic and alkaline in composition (nepheline-normative), and appear to have erupted through geochemically mature Precambrian crust, but have Sr and Nd isotope ratios that overlap broadly with the common sub-alkaline andesites and dacites at the volcanic front, where the volcanoes are underlain by geochemically immature oceanic terranes of Mesozoic age (Fig. 13). These observations, which indicate a limited role for geochemically mature continental crust in the genesis of modern lavas in Ecuador (see also Harmon *et al.*, 1984; James & Murcia, 1984), are supported by certain trace element ratios. In particular, Ba/La is variable and high in Ecuadoran lavas (similar to island arc basalts), but thus unlike lavas of the central and southern Andes, which have consistently low Ba/La, apparently as a result of assimilation of large quantities

of granitic crust (Fig. 11; Hildreth & Moorbath, 1988; Davidson *et al.*, 1990).

Arculus *et al.* (1999) pointed out that partial melting of a garnet-bearing mafic lower crust might explain the adakitic trace element patterns and relatively non-radiogenic isotope compositions observed in Ecuador andesites and dacites (see also Kilian *et al.*, 1994, 1995; Monzier *et al.*, 1999). Xenolith studies, combined with more recent work on the Raspas Metamorphic Complex, suggest that the deep crust beneath the volcanic front and main-arc areas should be a lithological mixture that spans a broad isotopic range from geochemically primitive/oceanic to geochemically mature and continental (Bosch *et al.*, 2002; Weber *et al.*, 2002). In particular, Weber *et al.* (2002) showed that deep crustal xenoliths from southern Colombia are unusually variable isotopically, with relatively radiogenic Pb (high  $^{207}\text{Pb}/^{204}\text{Pb}$ ) and a wide range in  $^{143}\text{Nd}/^{144}\text{Nd}$  compared with  $^{87}\text{Sr}/^{86}\text{Sr}$  (Figs 8 and 9). Similarly, Bosch *et al.* (2002) showed that the Raspas Metamorphic Complex includes eclogite-grade oceanic and continental lithologies which also span a large isotopic range (e.g.  $^{87}\text{Sr}/^{86}\text{Sr} = 0.7039\text{--}0.7226$ ). The highly variable isotopic composition of the deep crustal rocks (revealed in the Colombian xenoliths and Raspas Metamorphic Complex) is unlike that of the Ecuadoran lavas, which fall within an unusually narrow range, especially for  $^{143}\text{Nd}/^{144}\text{Nd}$  and  $^{87}\text{Sr}/^{86}\text{Sr}$  where they are offset only slightly (to more radiogenic  $^{87}\text{Sr}/^{86}\text{Sr}$ ) from the Galapagos Plume lavas (i.e. offset slightly from anticipated subducting plate compositions; Figs 8 and 9). It is likely that the andesites, dacites and rhyolites in Ecuador have assimilated some crust (e.g. Harmon *et al.*, 1984; James & Murcia, 1984; Bourdon *et al.*, 2003), but the highly variable and often radiogenic isotopic composition of the North Andean crust (based on the composition of the oceanic terranes, Colombian xenoliths and high-grade metamorphic terranes) suggests that it is not a major contributor to the source of Ecuadoran lavas. Again, this conclusion is reinforced by the cross-arc changes in isotopic compositions, which are small compared with the isotopic variability of the Ecuador crust, which changes from geochemically primitive oceanic terranes in the west to geochemically mature continental rock in the east.

It remains possible, of course, based on isotopic data alone, that partial melts of a newly underplated mafic layer at Moho depths (formed from basalts generated in the modern subduction zone and, therefore, isotopically similar to the modern arc lavas), could have contributed significantly to the source of the Ecuadoran lavas. Such an origin, which involves rapid remelting of a recently created (i.e. newly underplated) basaltic layer, has been proposed for Ecuador (Monzier *et al.*, 1999) and for other areas of thickened crust in the Andes, in particular in the case of the Miocene Cordillera Blanca Batholith in Peru (Petford & Atherton, 1996). At some level, this process

seems inevitable in any vigorously active magmatic arc. It is unlikely, however, that this process has exerted a major influence on magma genesis in the modern volcanic arc in Ecuador, where the lavas are mostly medium-K, calc-alkaline andesites whose major element compositions are unlike those of the silicic, alkali-rich, leucocratic granites that dominate the Cordillera Blanca in Peru ( $\text{SiO}_2 > 70\%$ ,  $\text{Na}_2\text{O} > 4\%$ ,  $\text{K}_2\text{O} > 3\%$ ,  $\text{MgO} < 2\%$ ,  $\text{FeO}^* < 2\%$ ). The latter appear to have formed by regional-scale melting of underplated basalt during the Miocene (Petford & Atherton, 1996). The rhyolites of Ecuador have major element compositions that are similar to the Cordillera Blanca leucogranites, but they constitute only a small proportion of the surface eruptive rocks, and unlike leucogranites from the Cordillera Blanca, the Ecuadoran rhyolites have relatively flat HREE patterns, which also contrast strongly with Cordillera Blanca mafic and intermediate rocks (e.g. compare Fig. 5 with Petford & Atherton, 1996, fig. 9).

Having emphasized that the crustal rocks of the northern Andes have played a limited role in the genesis of Ecuadoran lavas, compared with other parts of Andes where assimilation and wholesale melting of the crust appears to be common, it is important to point out that the Sr–Nd–Pb isotope systematics clearly indicate that, similar to the case in Colombia (James & Murcia, 1984), at least some assimilation of continental crust has affected many of the samples from Ecuador that we have analyzed. This is particularly clear from Pb and Nd isotope data, which are well correlated and appear to define mixing lines between Galapagos Plume–Carnegie Ridge basalts (i.e. probable subducting plate and mantle wedge compositions) and the local, geochemically mature continental crustal rocks (probable assimilants) that underlie many of the volcanoes in central Ecuador (Fig. 12). Bulk mixing calculations based on this Pb–Nd correlation indicate that most lavas in Ecuador contain no more than 5–10% of the local crust (Fig. 12). Assimilation of geochemically mature continental crustal material by the Ecuadoran lavas is well supported by the observed spatial–geochemical shifts in isotopic compositions across the arc, which reach maximum values for  $^{87}\text{Sr}/^{86}\text{Sr}$  and  $\Delta 7/4\text{Pb}$ , and minimum values for  $^{143}\text{Nd}/^{144}\text{Nd}$ , over the crest of the northern Andes in the main arc area at distances of 330–360 km from the trench (Fig. 13). Based on the high elevations and the presence of rhyolitic volcanism at Cotapaxi, Chalupas and Chacana, this area around the Inter-Andean depression appears to be the part of the Northern Andes where the crust is thickest, warmest, and where it is therefore most likely to contribute an assimilant to melts that are in transit from the subduction zone to the surface. Our estimate of the extent of the crustal contamination in Ecuadoran lavas, which is somewhat lower than some previous estimates (e.g. Kilian *et al.*, 1995; Barragan *et al.*, 1998), does not constrain the

possible role of geochemically primitive accreted oceanic terranes as a crustal assimilant, because those terranes are isotopically similar to the anticipated subducting plate and mantle wedge composition (Carnegie Ridge, Galapagos Plume, Figs 8 and 9).

The above interpretation implies that a significant proportion of the Ecuadoran lavas have remained unaffected or minimally affected by assimilation of geochemically mature continental crust (e.g. samples with  $\Delta 7/4\text{Pb} < 6.80$  and  $\epsilon\text{Nd} > 4.0$ , Figs 8 and 9). We cannot, of course, rule out the possibility that all of the lavas have been modified by assimilation of isotopically primitive crustal rocks, or that isotopically more primitive parental magmas were never erupted at the surface and, therefore, have not been sampled. We do not believe this is the case for two reasons. First, a large number of the Ecuadoran andesites and dacites have Pb, Sr and Nd isotopic compositions that are tightly clustered and partially overlap with (in Nd and Pb isotopes) likely subducting plate compositions in the form of Galapagos Plume and Carnegie Ridge basalts. This is similar to what is observed in many island arcs where the Pb, Nd and Sr isotopic compositions of the lavas approach those of MORB and are therefore widely believed to be controlled largely by geochemical components that originate in subducted MORB, marine sediment and seawater (Kay, 1980; Plank & Langmuir, 1993; Elliott *et al.*, 1997; Class *et al.*, 2000). Second, the alkali basalts and basaltic andesites at Sumaco, which appear, based on major and trace element compositions, to be low-percentage melts of mantle peridotite that has been less affected by subduction metasomatism than the associated andesites and dacites (Barragan *et al.*, 1998; Bourdon *et al.*, 2003), have extraordinarily high concentrations of Pb (12–29 ppm), Sr (>2000 ppm) and Nd (>80 ppm). Such high concentrations would have caused these melts to be much more resistant to isotopic modification during crustal assimilation compared with the andesites and dacites, which have lower concentrations of these elements, are more evolved (lower Mg-number) and were erupted at lower temperatures. Assuming that the more silicic and cooler lavas are more likely to have assimilated crust on their way to the surface (DePaolo, 1981), the broad isotopic overlap between the mafic alkaline lavas at Sumaco and the andesites and dacites implies that control over the composition of most Ecuadoran lavas lies primarily in the subduction zone, and not in the continental crust through which the melts passed (see also Barragan *et al.*, 1998; Bourdon *et al.*, 2003).

### Effects of crustal assimilation on trace elements

Ecuador andesites and dacites that have relatively high  $\Delta 7/4\text{Pb}$  and  $^{87}\text{Sr}/^{86}\text{Sr}$ , and low  $^{143}\text{Nd}/^{144}\text{Nd}$  (i.e. those

that appear to have assimilated a significant quantity of continental crust), generally have more variable and higher concentrations of the most incompatible trace elements, including Rb, Cs, Nb, Zr, Ba, Pb, and La. For example, as seen in Fig. 14, among the andesites and dacites with  $^{143}\text{Nd}/^{144}\text{Nd} < 0.51285$  ( $\epsilon\text{Nd} < 4.1$ ), four samples out of five have Zr > 100 ppm, whereas no sample with  $^{143}\text{Nd}/^{144}\text{Nd} > 0.51285$  has Zr > 100 ppm. A similar relationship can be seen in the Nb concentrations, which show a clear inverse correlation with  $^{143}\text{Nd}/^{144}\text{Nd}$ , but not for Y or Yb, where the elemental concentrations are not correlated with isotope ratios (Fig. 14). Not surprisingly, the rhyolites generally also have elevated concentrations of the highly incompatible elements and concomitantly higher  $^{87}\text{Sr}/^{86}\text{Sr}$  and  $\Delta 7/4\text{Pb}$ , and lower  $^{143}\text{Nd}/^{144}\text{Nd}$ , consistent with relatively higher degrees of crustal contamination (Fig. 14). For most incompatible elements, however, the correlation with isotopic composition is relatively weak.

Isotopic shifts attributable to crustal contamination are also accompanied by shifts in certain incompatible element ratios (Fig. 15). This is particularly clear for La/Yb, which is generally higher, and for Ba/La and Ba/Nb, which are generally lower in samples with relatively low  $^{143}\text{Nd}/^{144}\text{Nd}$  and high  $^{87}\text{Sr}/^{86}\text{Sr}$  (i.e. those that appear to have assimilated continental crust). These relationships suggest that cross-arc changes in La/Yb, Ba/Nb, etc., for the andesites and dacites are produced at least in part, by combined fractional crystallization and assimilation (AFC) of thickened continental crust, and not exclusively (as has been consistently argued in the literature) by increased depth and/or decreased percentage melting or by a decrease in the slab–fluid input to the mantle wedge. It is an important point, however, that the back-arc mafic and alkaline lavas at Sumaco (which anchor the cross-arc trends with high La/Yb and low Ba/Nb) retain the high  $^{143}\text{Nd}/^{144}\text{Nd}$  and low  $\Delta 7/4\text{Pb}$  that is characteristic of lavas at the volcanic front, and so do not appear to have been significantly modified by AFC processes (Fig. 13). We agree with the interpretation of the Sumaco lavas as deep, low-percentage, alkaline-series melts of mantle peridotite (Barragan *et al.*, 1998; Bourdon *et al.*, 2003), and emphasize that, as such, they represent relatively hot and dry melts with low viscosities, that are physically and chemically distinct from the felsic and intermediate-composition calc-alkaline lavas (andesite–dacite–rhyolite) that dominate volcanism in Ecuador.

In contrast to La/Yb and Ba/Nb, which appear to be significantly affected by crustal assimilation, the full range of Sr/Y observed in the Ecuador andesites and dacites appears to be present among samples with relatively primitive isotopic composition (e.g.  $^{143}\text{Nd}/^{144}\text{Nd} > 0.51285$ ,  $\Delta 7/4\text{Pb} < 7.0$ ; Fig. 15). This suggests that Sr/Y, a key ratio in the adakite characterization, is not substantially affected by crustal assimilation in andesite

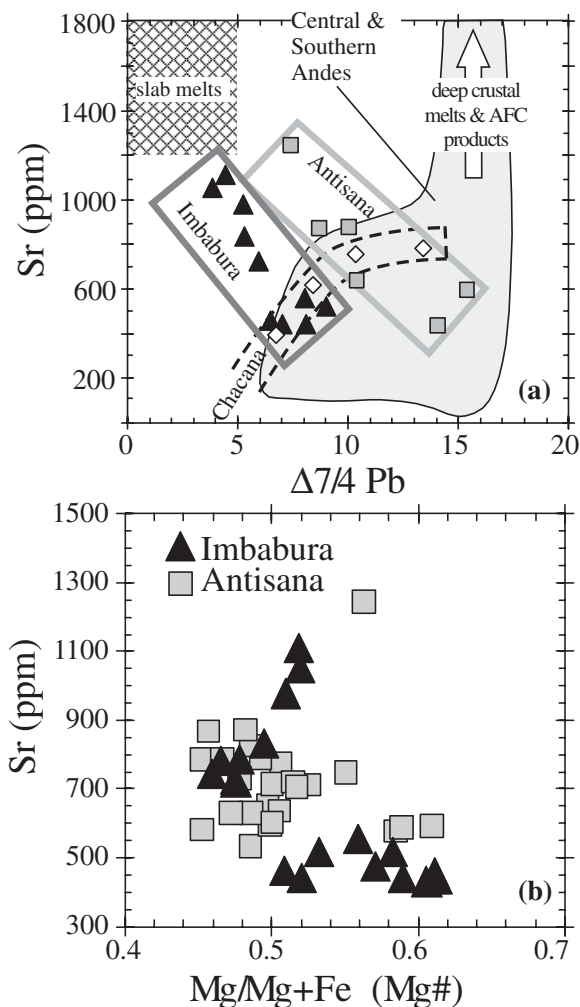


**Fig. 17.** (a) Sr concentration vs  $\Delta 7/4\text{Pb}$  showing trends at the Ecuador volcanic centers Imbabura, Antisana and Chacana; (b) Sr concentration vs Mg-number for Imbabura and Antisana. Data from Imbabura and Chacana are from Tables 1 and 2. Data from Antisana are from Tables 1 and 2 and from Bourdon *et al.* (2003). Slab melts (cross-hatched box) are presumed to contain high concentrations of Sr but relatively non-radiogenic Pb (e.g. Kay, 1978). Deep crustal melts and products of AFC (assimilation–fractional crystallization) in the Andes are presumed to contain relatively radiogenic Pb and possibly high concentrations of Sr (e.g. Garrison & Davidson, 2003).

and dacite lavas. In fact, for individual volcanoes where significant crustal assimilation has occurred, and where several andesite and dacite samples have been analyzed (e.g. Antisana, Imbabura), Sr/Y and Sr concentration appear to be inversely correlated with  $\Delta 7/4\text{Pb}$ , suggesting that, at some volcanoes, these quantities are highest in the samples that have assimilated the least amount of continental crust (Fig. 17).

We conclude that crustal assimilation has significantly changed the trace element abundances of some Ecuadorian lavas, but that assimilation does not play a clear and consistent role in the genesis of the adakitic trace

element characteristics, which are ubiquitous in the andesites and dacites in Ecuador.

### Origin of the ‘adakitic’ trace element characteristics in Ecuadorian lavas

Most andesites and dacites in Ecuador have REE characteristics that are adakitic; that is, they are enriched in the LREE, lack significant Eu anomalies, and are strongly fractionated between the middle REE (MREE) and HREE (Fig. 5). Unusually high concentrations of LREE in some Ecuadorian lavas may have been produced by assimilation of crustal rocks (as discussed above); however, assimilation alone cannot explain the low concentrations of Yb and Lu and the strongly fractionated MREE to HREE patterns (normalized  $\text{Gd/Yb} \gg 1.0$ ) that distinguish andesites and dacites in Ecuador from those in island arcs (Fig. 5d). Assuming that the melt source beneath the Northern Andes is approximately chondritic with respect to the HREE (i.e. normalized  $\text{Gd/Yb} \sim 1.0$ ), it is clear that garnet must have played a major role in the genesis of the Ecuadorian lavas. This role for garnet could be as a residual phase left after melt extraction or through removal by crystal fractionation under high pressures.

Several studies have concluded that garnet is involved in magma genesis beneath Ecuador when melting occurs at the surface of the subducting slab (e.g. Beate *et al.*, 2001; Bourdon *et al.*, 2002, 2003; Samaniego *et al.*, 2005). This is essentially an application of the Defant & Drummond (1990) adakite model in Ecuador. Among the lavas in Ecuador, those that appear to present the strongest case for the slab-melt interpretation have  $>700$  ppm Sr and relatively MORB-like isotopic compositions (Fig. 17). Lavas with these characteristics are well illustrated by our data from Imbabura Volcano, where there is a high-Sr liquid line of descent separate from the evolutionary pathway defined by lavas with 400–600 ppm Sr over the same range of  $\text{SiO}_2$  and Mg-number (Fig. 17). High-Sr lavas of this type appear to be present at Antisana Volcano (Fig. 17) and at Puñalica Volcano, where high Sr ( $>850$  ppm) and unradiogenic Sr isotopes ( $^{87}\text{Sr}/^{87}\text{Sr} < 0.7039$ ) define an end-member composition among the 23 samples from the Northern Andes studied by Harmon *et al.* (1984). Rocks of this geochemical type do not appear to exist among lavas of the central and southern Andes (Fig. 17) or in Colombia (James, 1982). In combination, these observations support the idea that melts from oceanic crust of the subducting Carnegie Ridge play a significant role in the genesis of at least some Ecuadorian lavas (Bourdon *et al.*, 2003, and references therein).

Despite the apparent control of the Carnegie Ridge on the surface expression of active volcanism in Ecuador (Fig. 1), and the clear presence of lavas with trace element



and isotopic compositions appropriate to the slab-melt interpretation (Fig. 17), the existence of thickened continental crust beneath Ecuador (at least 50 km; Prévot *et al.*, 1996; Guillier *et al.*, 2001) allows an alternative scenario by which adakite geochemistry may be produced, involving mantle melting and high-pressure crystal fractionation.

The presence of thick crust allows only a short column of mantle rock above the subduction zone (Fig. 1). This in turn means that melting within the mantle wedge will be relatively low percentage beneath Ecuador, compared with arcs in which the crust is thin and the melting column is long (Plank & Langmuir, 1988). In addition, we know from Sm/Nd and Lu/Hf systematics that melting in all of the major tectonic settings involves the stabilization of at least a small quantity of residual garnet (Salters, 1991; Hirschmann & Stolper, 1996). With these considerations in mind, it is reasonable to anticipate that Ecuador basalts, which are only rarely erupted in the volcanic front or main-arc areas, will generally have HREE patterns that are more strongly fractionated than those of common island arc basalts, which typically have Gd/Yb = 1.5–1.9 (e.g. Elliott *et al.*, 1997; George *et al.*, 2003). This expectation is confirmed by the few available analyses of basaltic rocks from Ecuador's main arc at Sangay Volcano, where four samples with SiO<sub>2</sub> < 54% have Gd/Yb = 2.6–3.2 (Monzier *et al.*, 1999), well within the range of the common Ecuadoran andesites and dacites, which typically have Gd/Yb = 2.0–3.7 (Table 1 and Samaniego *et al.*, 2005). These observations provide clear support for the idea that the physical conditions of melting within the mantle wedge beneath Ecuador may be conducive to the stabilization of small quantities of residual garnet and the formation of basaltic melts that have strongly fractionated trace element patterns with low Y and Yb.

Subsequent cooling and fractional crystallization in the deep crust beneath Ecuador are also likely to contribute to depletion of Y and HREE and enrichment in Sr to produce adakitic melts. This is true because basaltic to andesitic magmas with high H<sub>2</sub>O contents (5–6%) at pressures of 15–20 kbar (45–60 km depths) and at temperatures below 1100°C, will crystallize a mineral assemblage that is free of plagioclase and dominated by clinopyroxene and garnet ± amphibole (Green, 1972, 1982). Simple calculations using typical partition coefficients (McKenzie & O'Nions, 1991) demonstrate that if garnet constitutes 15–20% of the mineral assemblage, fractional crystallization will result in strongly compatible behavior for Y, Yb and Lu ( $D_{\text{BULK}} = 1.5\text{--}2.0$ ), progressively less compatible behavior for the MREE, and strongly incompatible behavior for La and Ce ( $D_{\text{BULK}} < 0.20$ ). This mechanism is clearly capable of producing the low concentrations of MREE to HREE that distinguish andesites and dacites in Ecuador from lavas of

similar major element compositions produced in island arcs (Fig. 5d). These physical conditions for melt evolution (high-pressure and hydrous) will also suppress crystallization of plagioclase (Green, 1982), which in turn will cause Sr to behave as an incompatible element that can be enriched to high concentration as the melts evolve by crystal fractionation. The experimental studies of Green (1972, 1982) have similarly demonstrated that the major element character of the calc-alkaline series (basalt, andesite, dacite) can be explained by crystal fractionation processes under high-pressure and hydrous condition (see also Hildreth & Moorbath, 1988; Garrison & Davidson, 2003).

More broadly, the deep crustal fractionation mechanism is consistent with the basic observation that the trace element characteristics of Ecuadoran lavas are highly variable, even though their Pb, Sr and Nd isotopic compositions are relatively primitive and homogeneous. This is true for lavas throughout Ecuador, and within individual volcanoes (Samaniego *et al.*, 2002, 2005), and is consistent with the idea that melt batches may evolve by crystal fractionation to create either 'adakitic' or 'classic calc-alkaline' trace element characteristics, dependent on the depth/pressure of fractionation, and consequently on the presence or absence of garnet in the fractionating assemblage.

The history of magmatism in Ecuador since the Eocene appears most consistent with the deep crustal fractionation model. Chiaradia *et al.* (2004) recently showed that Eocene to Late Miocene andesites in Ecuador (50–9 Ma) have relatively flat REE patterns that contrast with the younger, Miocene to Recent lavas, which are adakitic (see Chiaradia *et al.*, 2004, fig. 8). The differences in REE characteristics imply that different processes operated in the genesis of these lavas of different ages. Available Pb isotope data, however, indicate that the magma source region beneath Ecuador has remained largely unchanged since the Eocene. Chiaradia *et al.* (2004) argued that these observations imply that the magmatic plumbing systems beneath Ecuador shifted to depths within the stability field of garnet after ~9 Ma, probably in response to a crustal thickening event, possibly caused by the initial collision and subduction of the Carnegie Ridge. The alternative interpretation involves a shift in source from the mantle wedge to the subducting plate at the point in time when subduction of the Carnegie Ridge began (i.e. Bourdon *et al.*, 2003, and references therein). This alternative remains possible, but appears less likely in the light of the new isotopic data, which suggest that the melt source beneath Ecuador has remained approximately constant since the Eocene (Chiaradia *et al.*, 2004).

One weakness of the deep crustal fractionation model described here for adakite genesis is that it requires fractional crystallization of garnet, even though garnet phenocrysts are not observed in Ecuadoran lavas.

Garnets are not commonly found as phenocrysts in calc-alkaline lavas; they are, however, known from several localities and their potential role in the evolution of andesitic and dacitic lavas is well documented experimentally (Green & Ringwood, 1968; Fitton, 1972; Green, 1972, 1982; Hamer & Moyes, 1982; Day *et al.*, 1992). If the deep crustal fractionation model is correct, this means simply that the plagioclase–pyroxene–amphibole phenocryst assemblage in the Ecuadoran lavas is produced late in the magmatic evolution, during magma storage in shallow-level systems where garnet is unstable (e.g. Fitton, 1972).

## CONCLUSIONS

(i) Primitive and relatively homogeneous Sr, Nd and Pb isotopic compositions indicate that lavas throughout Ecuador are produced largely within the supra-subduction zone mantle wedge and not by extensive melting of the North Andean crust.

(ii) Changes in  $^{143}\text{Nd}/^{144}\text{Nd}$ ,  $\Delta 7/4\text{Pb}$  and La/Yb across the arc in Ecuador are interpreted to result from assimilation of geochemically mature continental crust, especially in the main-arc area, at distances of 330–360 km from the trench. Mixing calculations limit the quantity of assimilated continental crust to less than ~10%.

(iii) Possible assimilation of geochemically primitive crustal rock beneath the Western Cordillera remains poorly constrained; however, assimilation of crustal rocks does not appear to play a clear and consistent role in the genesis of the adakitic trace element patterns that are common in andesites and dacites in Ecuador.

(iv) Available whole-rock data do not provide a clear basis for distinguishing between slab-melting and deep crustal fractionation models for the genesis of adakitic lavas in Ecuador. Both models derive adakites from basalt, either by partial melting or fractional crystallization, and both explain the observed fractionation of REE patterns with garnet. None the less, the geochemical evolution within individual volcanoes (Samaniego *et al.*, 2005), and in magmatic rocks produced throughout Ecuador since the Eocene (Chiaradia *et al.*, 2004), appears to favor the deep crustal fractionation model for the genesis of most post-Miocene lavas in Ecuador.

## ACKNOWLEDGEMENTS

This paper benefited substantially from thoughtful reviews by Henrietta Lapierre, Erwan Bourdon, Pablo Samaniego and Jennifer Garrison. We thank Nick Arndt and Marjorie Wilson for their thoughtful, thorough and timely handling of this work. Thanks also go to Drew Coleman for his assistance in acquiring the isotopic data.

This paper also benefited from discussions with members of the University of South Carolina Solid-Earth Group. We thank in particular Jim Kellogg, Matt Kohn, Jim Knapp, and Bob Trenkamp. Thanks also go to Dennis Geist and Roberto Barragan, who generously provided samples from Sumaco, Antisana and Atacazo for this study, and to Sue Kay for many helpful discussions regarding Andean petrology and geochemistry.

## REFERENCES

- Abratis, M. & Wörner, G. (2001). Ridge collision, slab-window formation, and the flux of Pacific asthenosphere into the Caribbean realm. *Geology* **29**, 127–130.
- Arculus, R. J., Lapierre, H. & Jaillard, E. (1999). Geochemical window into subduction and accretion processes: Rapas metamorphic complex, Ecuador. *Geology* **27**, 547–550.
- Aspden, J. A. & Litherland, M. (1992). The geology and Mesozoic collisional history of the Cordillera Real, Ecuador. *Tectonophysics* **205**, 187–204.
- Aspden, J. A., Harrison, S. H. & Rundle, C. C. (1992). New geochronological control for the tectono-magmatic evolution of the metamorphic basement, Cordillera Real and El Oro Province of Ecuador. *Journal of South American Earth Sciences* **6**, 77–96.
- Atherton, M. P. & Petford, N. (1993). Generation of sodium-rich magmas from newly underplated basaltic crust. *Nature* **362**, 144–146.
- Barazangi, M. & Isacks, B. (1976). Spatial distribution of earthquakes and subduction of the Nazca plate beneath South America. *Geology* **4**, 686–692.
- Barragan, R., Geist, D., Hall, M., Larsen, P. & Kurz, M. (1998). Subduction controls on the compositions of lavas from the Ecuadorian Andes. *Earth and Planetary Science Letters* **154**, 153–166.
- Beate, B., Monzier, M., Spikings, R., Cotten, J., Silva, J., Bourdon, E. & Eissen, J. P. (2001). Mio-Pliocene adakite generation related to flat subduction in southern Ecuador: the Quimsacocha volcanic center. *Earth and Planetary Science Letters* **192**, 561–570.
- Ben Othman, D., White, W. M. & Patchett, J. (1989). The geochemistry of marine sediments, island arc magma genesis, and crust–mantle recycling. *Earth and Planetary Science Letters* **94**, 1–21.
- Bosch, D., Piercarlo, G., Lapierre, H., Malfere, J. & Jaillard, E. (2002). Geodynamic significance of the Rapas Metamorphic Complex (SW Ecuador): geochemical and isotopic constraints. *Tectonophysics* **345**, 83–102.
- Bourdon, E., Eissen, J. P., Monzier, M., Robin, C., Martin, H., Cotten, J. & Hall, M. L. (2002). Adakite-like lavas from Antisana Volcano (Ecuador): evidence for slab melt metasomatism beneath Andean Northern Volcanic Zone. *Journal of Petrology* **43**, 199–217.
- Bourdon, E., Eissen, J. P., Gutscher, M. A., Monzier, M., Hall, M. L. & Cotten, J. (2003). Magmatic response to early aseismic ridge subduction: the Ecuadorian margin case (South America). *Earth and Planetary Science Letters* **205**, 123–138.
- Calvache, M. L. & Williams, S. N. (1997). Geochemistry and petrology of the Galeras Volcanic Complex, Colombia. *Journal of Volcanology and Geothermal Research* **77**, 21–38.
- Chiaradia, M., Fontboté, L. & Beate, B. (2004). Cenozoic continental arc magmatism and associated mineralization in Ecuador. *Mineralium Deposita* **39**, 204–222.
- Class, C., Miller, D. M., Goldstein, S. L. & Langmuir, C. H. (2000). Distinguishing melt and fluid subduction components in Umnak

- Volcanics, Aleutian Arc. *Geochemistry, Geophysics, Geosystems* 1999GC000010.
- Conrad, W. K. & Kay, R. W. (1984). Ultramafic and mafic inclusions from Adak Island: crystallization history, and implications for the nature of primary magmas and crustal evolution in the Aleutian arc. *Journal of Petrology* **25**, 88–125.
- Davidson, J. P. (1987). Crustal contamination versus subduction zone enrichment: examples from the Lesser Antilles and implications for mantle source compositions of island arc volcanic rocks. *Geochimica et Cosmochimica Acta* **51**, 2185–2198.
- Davidson, J. P., Ferguson, K. M., Colucci, M. T. & Dungan, M. A. (1988). The origin and evolution of magmas from the San Pedro–Pellado Volcanic Complex, S. Chile: multicomponent sources and open system evolution. *Contributions to Mineralogy and Petrology* **100**, 425–445.
- Davidson, J. P., McMillan, N. J., Moorbath, S., Wörner, G., Harmon, R. S. & Lopez-Escobar, L. (1990). The Nevados de Payachata volcanic region (18°S/69°W, N. Chile); II, Evidence for widespread crustal involvement in Andean magmatism. *Contributions to Mineralogy and Petrology* **105**, 412–432.
- Day, R. A., Green, T. H. & Smith, I. E. M. (1992). The origin and significance of garnet phenocrysts and garnet-bearing xenoliths in Miocene calc-alkaline volcanics from Northland, New Zealand. *Journal of Petrology* **33**, 125–161.
- Defant, M. J. & Drummond, M. S. (1990). Derivation of some modern arc magmas by melting of young subducted lithosphere. *Nature* **347**, 662–665.
- Defant, M. J., Richerson, P. M., De Boer, J. Z., Stewarta, R. H., Maury, R. C., Bellon, H., Drummond, M. S., Feigenson, M. D. & Jackson, T. E. (1991). Dacite genesis via both slab melting and differentiation: petrogenesis of La Yeguada Volcanic Complex, Panama. *Journal of Petrology* **32**, 1101–1142.
- DePaolo, D. J. (1981). Trace element and isotopic effects of combined wallrock assimilation and fractional crystallization. *Earth and Planetary Science Letters* **53**, 189–202.
- Deruelle, B. (1982). Petrology of the Plio-Quaternary volcanism of the south-central and meridional Andes. *Journal of Volcanology and Geothermal Research* **14**, 77–124.
- Dickinson, W. R. (1975). Potash–depth (*K–h*) relations in continental margin and intra-oceanic magmatic arcs. *Geology* **3**, 53–56.
- Droux, A. & Delaloye, M. (1996). Petrography and geochemistry of Plio-Quaternary calc-alkaline volcanoes of southwestern Colombia. *Journal of South American Earth Sciences* **9**, 27–41.
- Dupré, B. & Echeverría, L. M. (1984). Pb isotopes of Gorgona Island (Colombia): isotopic variations correlated with magma type. *Earth and Planetary Science Letters* **67**, 186–190.
- Elliott, T., Plank, T., Zindler, A., White, W. & Bourdon, B. (1997). Element transport from slab to volcanic front at the Mariana arc. *Journal of Geophysical Research* **102**, p. 14991–15091.
- Ewart, E. (1982). The mineralogy and petrology of Tertiary–Recent orogenic volcanic rocks with special reference to the andesite–basaltic composition range. In: Thorpe, R. S. (ed.) *Orogenic Andesites and Related Rocks*, New York: John Wiley, pp. 25–87.
- Feininger, T. (1987). Allochthonous terranes in the Andes of Ecuador and northwestern Peru. *Canadian Journal of Earth Science* **24**, 266–278.
- Feininger, T. & Seguin, M. K. (1983). Bouguer gravity anomaly field and inferred crustal structure of continental Ecuador. *Geology* **11**, 40–44.
- Fitton, J. G. (1972). The genetic significance of almandine–pyrope phenocrysts in the calc-alkaline Borrowdale Volcanic Group, Northern England. *Contributions to Mineralogy and Petrology* **36**, 231–248.
- Frey, F. A., Gerlach, D. C., Hickey, R. L., Lopez-Escobar, L. & Munizaga-Villavicencio, F. (1984). Petrogenesis of the Laguna del Maule volcanic complex, Chile (36°S). *Contributions to Mineralogy and Petrology* **88**, 133–149.
- Futa, K. & Stern, C. R. (1988). Sr and Nd isotopic and trace element compositions of Quaternary volcanic centers of the southern Andes. *Earth and Planetary Science Letters* **88**, 253–262.
- Garrison, J. M. & Davidson, J. P. (2003). Dubious case for slab melting in the Northern volcanic zone of the Andes. *Geology* **31**, 565–568.
- George, R., Turner, S., Hawkesworth, C. J., Morris, J., Nye, C., Ryan, J. G. & Zheng, S.-H. (2003). Melting processes and fluid and sediment transport rates along the Alaska–Aleutian arc from an integrated U–Th–Ra–Be isotope study. *Journal of Geophysical Research* **108**, 1–25.
- Gerlach, D. C., Frey, F. A., Moreno-Roa, H. & Lopez-Escobar, L. (1988). Recent volcanism in the Puyehue–Cordon Daulle region, Southern Andes, Chile (40–5°S); petrogenesis of evolved lavas. *Journal of Petrology* **29**, 333–382.
- Gill, J. (1981). *Orogenic Andesites and Plate Tectonics*. New York: Springer.
- Graindorge, D., Calahorrano, A., Charvis, P., Collot, J. Y. & Bethoux, N. (2004). Deep structure of the Ecuador convergent margin and the Carnegie Ridge, possible consequences on great earthquakes recurrence interval. *Geophysical Research Letters* **31**, 10.1029/2003GL018803.
- Green, T. H. (1972). Crystallization of calc-alkaline andesite under controlled high-pressure hydrous conditions. *Contributions to Mineralogy and Petrology* **34**, 150–166.
- Green, T. H. (1982). Anatexis of mafic crust and high pressure crystallization of andesite. In: Thorpe, R. S. (ed.) *Orogenic Andesites and Related Rocks*, New York: John Wiley, pp. 465–487.
- Green, T. H. & Ringwood, A. E. (1968). Origin of garnet phenocrysts in calc-alkaline rocks. *Contributions to Mineralogy and Petrology* **18**, 163–174.
- Guillier, B., Chatelain, J. L., Jaillard, E., Yepes, H., Poupinet, G. & Fels, J. F. (2001). Seismological evidence on the geometry of the orogenic system in central–northern Ecuador (South America). *Geophysical Research Letters* **28**, 3749–3752.
- Gutscher, M. A., Malavieille, J., Lallemand, S. & Collot, J. Y. (1999). Tectonic segmentation of the North Andean margin: impact of the Carnegie Ridge collision. *Earth and Planetary Science Letters* **168**, 255–270.
- Gutscher, M. A., Maury, R. C., Eissen, J. P. & Bourdon, E. (2000). Can slab melt be caused by flat slab? *Geology* **28**, 535–538.
- Hamer, R. D. & Moyes, A. B. (1982). Composition and origin of garnet from the Antarctic Peninsula Volcanic Group of Trinity Peninsula. *Journal of the Geological Society, London* **139**, 713–720.
- Harmon, R. S., Barreiro, B., Moorbath, S., Hoefs, J., Francis, P. W., Thorpe, R. S., Deruelle, B., McHugh, J. & Viglino, J. A. (1984). Regional O-, Sr-, and Pb-isotope relationships in the late Cenozoic calc-alkaline lavas of the Andean Cordillera. *Journal of the Geological Society, London* **141**, 803–822.
- Harpp, K. S. & White, W. M. (2001). Tracing a mantle plume: isotopic and trace element variations of Galapagos seamounts. *Geochemistry, Geophysics, Geosystems* 2000GC000137.
- Hart, S. R. (1984). A large-scale isotope anomaly in the Southern Hemisphere mantle. *Nature* **309**, 753–757.
- Hauff, F., Hoernle, K., van den Bogaard, P., Alvarado, G. & Garbe-Schönberg, D. (1999). Age and geochemistry of basaltic complexes in western Costa Rica: contributions to the geotectonic evolution of Central America. *Geochemistry, Geophysics, Geosystems* 1999GC000020.
- Hauff, F., Hoernle, K., Tilton, G., Graham, D. W. & Kerr, A. C. (2000). Large volume recycling of oceanic lithosphere over short time scales: geochemical constraints from the Caribbean Large Igneous Province. *Earth and Planetary Science Letters* **174**, 247–263.

- Hickey, R. L., Frey, F. & Gerlach, D. C. (1986). Multiple sources for basaltic arc rocks from the southern volcanic zone of the Andes (34–41S): trace element and isotopic evidence for contributions from subducted oceanic crust, mantle, and continental crust. *Journal of Geophysical Research* **91**, 5963–5983.
- Hildreth, W. & Moorbath, S. (1988). Crustal contributions to arc magmatism in the Andes of central Chile. *Contributions to Mineralogy and Petrology* **98**, 455–489.
- Hirschmann, M. M. & Stolper, E. M. (1996). A possible role for garnet pyroxenite in the origin of the ‘garnet signature’ in MORB. *Contributions to Mineralogy and Petrology* **124**, 185–208.
- Hörmann, P. K. & Pichler, H. (1982). Geochemistry, petrology and origin of the Cenozoic volcanic rocks of the Northern Andes in Ecuador. *Journal of Volcanology and Geothermal Research* **12**, 259–282.
- Hughes, R. A. & Pilatasig, L. F. (2002). Cretaceous and Tertiary terrane accretion in the Cordillera Occidental of the Andes of Ecuador. *Tectonophysics* **345**, p. 29–48.
- Jaillard, E., Soler, P., Carlier, G. & Mourier, T. (1990). Geodynamic evolution of the northern and central Andes during early-to-middle Mesozoic times: a Tethyan model. *Journal of the Geological Society, London* **147**, 1009–1022.
- Jaillard, E., Benítez, S. & Mascle, G. H. (1997). Les déformations paléogènes de la zone d’avant-arc sud-équatorienne en relation avec l’évolution géodynamique. *Bulletin de la Société Géologique de France* **168**, 403–412.
- James, D. E. (1982). A combined O, Sr, Nd, and Pb isotopic and trace element study of crustal contamination in central Andean lavas, I. Local geochemical variations. *Earth and Planetary Science Letters* **57**, 47–62.
- James, D. E. & Murcia, L. A. (1984). Crustal contamination in northern Andean volcanics. *Journal of the Geological Society, London* **141**, 823–830.
- Johnson, D. M., Hooper, P. R. & Conrey, R. M. (1999). XRF analysis of rocks and minerals for major and trace elements on a single low-dilution Li-tetraborate fused bead. *Advances in X-ray Analysis* **41**, 117–132.
- Kay, R. W. (1978). Aleutian magnesian andesites: melts from subducted Pacific oceanic crust. *Journal of Volcanology and Geothermal Research* **4**, 117–132.
- Kay, R. W. (1980). Volcanic arc magma genesis: implications for element recycling in the crust–upper mantle system. *Journal of Geology* **88**, 497–522.
- Kay, R. W. & Kay, S. M. (1991). Creation and destruction of lower continental crust. *Geologische Rundschau* **80**, 259–278.
- Kay, S. M., Ramos, V. A. & Marquez, Y. M. (1993). Evidence in Cerro Pampa volcanic rocks for slab-melting prior to ridge–trench collision in southern South America. *Journal of Geology* **101**, 703–714.
- Kelemen, P. B. (1995). Genesis of high Mg# andesites and the continental crust. *Contributions to Mineralogy and Petrology* **120**, 1–19.
- Kelemen, P. B., Yogodzinski, G. M. & Scholl, D. W. (2003). Along-strike variation in lavas of the Aleutian Island Arc: implications for the genesis of high Mg# andesite and the continental crust. In: Eiler, J. (ed.) *Inside the Subduction Factory*, Geophysical Monograph 138, Washington, DC: American Geophysical Union, pp. 223–276.
- Kerr, A. C. & Tarney, J. (2005). Tectonic evolution of the Caribbean and northwestern South America: the case for accretion of two Late Cretaceous oceanic plateaus. *Geology* **33**, 269–272.
- Kerr, A. C., Tarney, J., Marriner, G. F., Nivia, A. & Saunders, A. D. (1996). The geochemistry and tectonic setting of Late Cretaceous Caribbean and Colombian volcanism. *Journal of South American Earth Sciences* **9**, 111–120.
- Kerr, A. C., Marriner, G. F., Tarney, J., Nivia, A., Saunders, A. D. & Thirlwall, M. F. (1997). Cretaceous basaltic terranes in western Colombia; elemental, chronological and Sr–Nd isotopic constraints on petrogenesis. *Journal of Petrology* **38**, 677–702.
- Kerr, A. C., Tarney, J., Kempton, P. D., Spadea, P., Nivia, A., Marriner, G. F. & Duncan, R. A. (2002). Pervasive mantle plume head heterogeneity: evidence from the late Cretaceous Caribbean–Colombian oceanic plateau. *Journal of Geophysical Research* **107**(B7), 10.1029/2001JB000790.
- Kerr, A. C., Tarney, J., Kempton, P. D., Pringle, M. S. & Nivia, A. (2004). Mafic pegmatites intruding oceanic plateau gabbros and ultramafic cumulates from Bolivar, Colombia: evidence for a ‘wet’ mantle plume? *Journal of Petrology* **45**, 1877–1906.
- Kilian, R. & Pichler, H. (1989). The North Andean volcanic zone. *Zentralblatt für Geologie und Paläontologie, Teil I* **5/6**, 1075–1085.
- Kilian, R., Hegner, E., Fortier, S. & Satir, M. (1994). The genesis of Quaternary volcanic rocks in contrasting lithospheric settings of Ecuador. *7th Chilean Geologic Congress Abstracts* **2**, 1378–1382.
- Kilian, R., Hegner, E., Fortier, S. & Satir, M. (1995). Magma evolution within the accretionary mafic basement of Quaternary Chimborazo and associated volcanos (Western Ecuador). *Revista Geologica de Chile* **22**, 203–208.
- Lapierre, H., Bosch, D., Dupuis, V., Polvé, M., Maury, R. C., Hernandez, J., Monié, P., Yeghicheyan, D., Jaillard, E., Tardy, M., de Lépinay, B. M., Mamberti, M., Desmet, A., Keller, F. & Sénebier, F. (2000). Multiple plume events in the genesis of the peri-Caribbean Cretaceous oceanic plateau province. *Journal of Geophysical Research* **105**, 8403–8421.
- Lichte, F. E., Meier, A. L. & Crock, J. G. (1987). Determination of rare-earth elements in geological materials by inductively coupled plasma mass spectrometry. *Analytical Chemistry* **59**, 1150–1157.
- Litherland, M., Aspden, J. A. & Jemielita, R. A. (1994). *The Metamorphic Belts of Ecuador*. Keyworth: British Geological Survey.
- Lopez-Escobar, L. (1984). *Andean Magmatism: Chemical and Isotopic Constraints*, Shiva Publishing, Nantwich, UK. *Petrology and Chemistry of Volcanic Rocks of the Southern Andes*, pp. 47–71.
- Lopez-Escobar, L., Frey, F. A. & Vergara, M. (1977). Andesites and high-alumina basalts from the central–south Chile High Andes; geochemical evidence bearing on their petrogenesis. *Contributions to Mineralogy and Petrology* **63**, 199–228.
- Lopez-Escobar, L., Moreno, H., Tagiri, M., Notsu, K. & Onuma, N. (1985). Geochemistry and petrology of lavas from San Jose Volcano, Southern Andes (33°45’S). *Geochemical Journal* **19**, 209–222.
- Lugnair, G. W. & Carlson, R. W. (1978). The Sm–Nd history of KREEP. *Proceedings of the 9th Lunar and Planetary Science Conference. Geochimica et Cosmochimica Acta Supplement*, 689–704.
- Mamberti, M., Lapierre, H., Bosch, D., Jaillard, E., Ethien, R., Hernandez, J. & Polvé, M. (2003). Accreted fragments of the Late Cretaceous Caribbean–Colombian Plateau in Ecuador. *Lithos* **66**, 173–199.
- McKenzie, D. & O’Nions, R. K. (1991). Partial melt distributions from inversion of rare earth element concentrations. *Journal of Petrology* **32**, 1021–1091.
- Megard, F. (1989). The evolution of the Pacific Ocean margin in South America north of Arica elbow (18°S). In: Ben Avraham, Z. (ed.) *Oxford Monographs on Geology and Geophysics, No. 8*. New York: Oxford University Press, pp. 208–230.
- Miyashiro, A. (1974). Volcanic rock series in island arcs and active continental margins. *American Journal of Science* **274**, 321–355.
- Monzier, M., Robin, C., Samaniego, P., Hall, M. L., Cotten, J., Mothes, P. & Arnaud, N. (1999). Sangay Volcano, Ecuador: structural development, present activity and petrology. *Journal of Volcanology and Geothermal Research* **90**, 49–79.

- Morris, P. A. (1995). Slab melting as an explanation of Quaternary volcanism and aseismicity in southwest Japan. *Geology* **23**, 395–398.
- Noble, S. R., Aspden, J. A. & Jemielita, R. A. (1997). Northern Andean crustal evolution: new U–Pb geochronological constraints from Ecuador. *Geological Society of America Bulletin* **109**, 789–798.
- Petford, N. & Atherton, M. (1996). Na-rich partial melts from newly underplated basaltic crust: the Cordillera Blanca Batholith, Peru. *Journal of Petrology* **37**, 1491–1521.
- Pichler, J., Hörmann, P. K. & Braun, A. F. (1976). First petrologic data on lavas of the Volcano El Reventador (Eastern Ecuador). *Münstersche Forschungen zur Geologie und Paläontologie* **38**, 129–141.
- Plank, T. & Langmuir, C. H. (1988). An evaluation of the global variations in the major element chemistry of arc basalts. *Earth and Planetary Science Letters* **90**, 349–370.
- Plank, T. & Langmuir, C. H. (1993). Tracing trace elements from sediment input to volcanic output at subduction zones. *Nature* **362**, 739–742.
- Prévoit, R., Chatelain, J.-L., Guillier, B. & Yepes, H. (1996). Tomographie des Andes Equatoriennes: évidence d'une continuité des Andes Centrales. *Comptes Rendus de l'Académie des Sciences, Série II. Sciences de la Terre et des Planètes* **323**, 833–840.
- Rapp, R. P., Shimizu, N., Norman, M. D. & Applegate, G. S. (1999). Reaction between slab-derived melts and peridotite in the mantle wedge: experimental constraints at 3–8 GPa. *Chemical Geology* **160**, 335–356.
- Reynaud, C., Jaillard, E. & Lapierre, H. (1999). Oceanic plateau and island arcs of SW Ecuador: their place in the geodynamic evolution of northwestern South America. *Tectonophysics* **307**, 235–254.
- Salters, V. J. M. (1991). The mantle sources of ocean ridges, islands and arcs: the Hf-isotope connection. *Earth and Planetary Science Letters* **104**, 364–380.
- Salvador, M.E. (1991). Gravity Field, Topography and Crustal Structure of the North Andes, University of South Carolina Department of Geological Sciences Masters Thesis, Columbia, SC, 100 pp.
- Samaniego, P., Martin, H., Robin, C. & Monzier, M. (2002). Transition from calc-alkalic to adakitic magmatism at Cayambe volcano, Ecuador: insights into slab melts and mantle wedge interactions. *Geology* **30**, 967–970.
- Samaniego, P., Martin, H., Monzier, M., Robin, C., Fornari, M., Eissen, J. P. & Cotten, J. (2005). Temporal evolution of magmatism in the Northern Volcanic Zone of the Andes: the geology and petrology of Cayambe Volcanic Complex (Ecuador). *Journal of Petrology* **46**, 2225–2252.
- Saunders, A. D., Rogers, G., Marriner, G. F., Terrell, D. J. & Verma, S. P. (1987). Geochemistry of Cenozoic volcanic rocks, Baja California, Mexico: implications for the petrogenesis of post-subduction magmas. *Journal of Volcanology and Geothermal Research* **32**, 223–245.
- Sigurdsson, H., Carey, S., Palais, J. M. & Devine, J. (1990). Pre-eruption compositional gradients and mixing of andesite and dacite magma erupted from Nevado del Ruiz Volcano, Colombia in 1985. *Journal of Volcanology and Geothermal Research* **41**, 127–151.
- Singer, B. S. & Myers, J. D. (1990). Intra-arc extension and magmatic evolution in the central Aleutian arc, Alaska. *Geology* **18**, 1050–1053.
- Stern, C. R. & Killian, R. (1996). Role of the subducted slab, mantle wedge and continental crust in the generation of adakites from the Andean Austral Volcanic Zone. *Contributions to Mineralogy and Petrology* **123**, 263–281.
- Sun, S. S. & McDonough, W. F. (1989). Chemical and isotopic systematics of oceanic basalts: implications for mantle composition and processes. In: Saunders, A. D. & Norry, M. J. (eds) *Magmatism in the Ocean Basins. Geological Society, London, Special Publications* **42**, 313–346.
- Tanaka, T., Togashi, S., Kamioka, H., Amakawa, H., Kagami, H., Hamamoto, T., Yuhara, M., Orihashi, Y., Yoneda, S., Shimizu, H., Kunimaru, T., Takahashi, K., Yanagi, Y., Nakano, T., Fujimaki, H., Shinjo, R., Asahara, Y., Tanimizu, M. & Dragusanu, C. (2000). JNdi-1: a neodymium isotopic reference in consistency with La Jolla neodymium. *Chemical Geology* **168**, 279–281.
- Thorpe, R. S., Francis, P. W. & O'Callaghan, L. (1983). Relative roles of source composition, fractional crystallization and crustal contamination in the petrogenesis of Andean volcanic rocks. *Philosophical Transactions of the Royal Society of London, Series A* **310**, 675–692.
- Trenkamp, R., Kellogg, J. N., Freymueller, J. T. & Mora, H. P. (2002). Wide plate margin deformation, southern Central America and northwestern South America, CASA GPS observations. *Journal of South American Earth Sciences* **15**, 157–171.
- Vanek, J., Vankova, V. & Hanus, V. (1994). Geochemical zonation of volcanic rocks and deep structure of Ecuador and southern Colombia. *Journal of South American Earth Sciences* **7**, 57–67.
- Walker, J. A., Moulds, T. N., Zentilli, M. & Feigenson, M. D. (1991). Spatial and temporal variations in volcanics of the Andean central volcanic zone (26 to 28°S). In: Harmon, R. S. & Rapela, C. W. (eds) *Andean Magmatism and its Tectonic Setting, Geological Society of America Special Paper 265*, Geological Society of America, Boulder, CO, U.S.A.: pp. 139–155.
- Wasserburg, G. J., Jacobsen, S. B., DePaolo, D. J., McCulloch, M. T. & Wen, T. (1981). Precise determination of Sm/Nd ratios, Sm and Nd isotopic abundances in standard solutions. *Geochimica et Cosmochimica Acta* **45**, 2311–2323.
- Weber, M. B. I., Tarney, J., Kempton, P. D. & Kent, R. W. (2002). Crustal make-up of the northern Andes: evidence based on deep crustal xenolith suites, Mercaderes, SW Colombia. *Tectonophysics* **345**, 49–82.
- Werner, R., Hoernle, K., Barckhausen, U. & Hauff, F. (2003). Geodynamic evolution of the Galapagos hot spot system (Central East Pacific) over the past 20 m.y.: constraints from morphology, geochemistry and magnetic anomalies. *Geochemistry, Geophysics, Geosystems* 2003GC000576.
- White, W. M., McBirney, A. R. & Duncan, R. A. (1993). Petrology and geochemistry of the Galapagos Islands: portrait of a pathological mantle plume. *Journal of Geophysical Research* **98**, 19533–19563.
- Woodhead, J. D. (1988). The origin of geochemical variations in Mariana lavas: a general model for petrogenesis in intra-oceanic island arcs? *Journal of Petrology* **29**, 805–830.
- Wörner, G. (1989). The Nevados de Payachata volcanic region (18°S/69°W, N. Chile). *Bulletin of Volcanology* **50**, 287–303.
- Yogodzinski, G. M., Kay, R. W., Volynets, O. N., Koloskov, A. V. & Kay, S. M. (1995). Magnesian andesite in the western Aleutian Komandorsky region: implications for slab melting and processes in the mantle wedge. *Geological Society of America Bulletin* **107**, 505–519.
- Zartman, R. E. & Haines, S. M. (1988). The plumbotectonic model for Pb isotopic systematics among major terrestrial reservoirs—a case for bi-directional transport. *Geochimica et Cosmochimica Acta* **52**, 1327–1339.